Numerical modelling of morphodynamics —Vilaine Estuary

Hans Jacob Vested, Caroline Tessier, Bo Brahtz Christensen & Evelyne Goubert

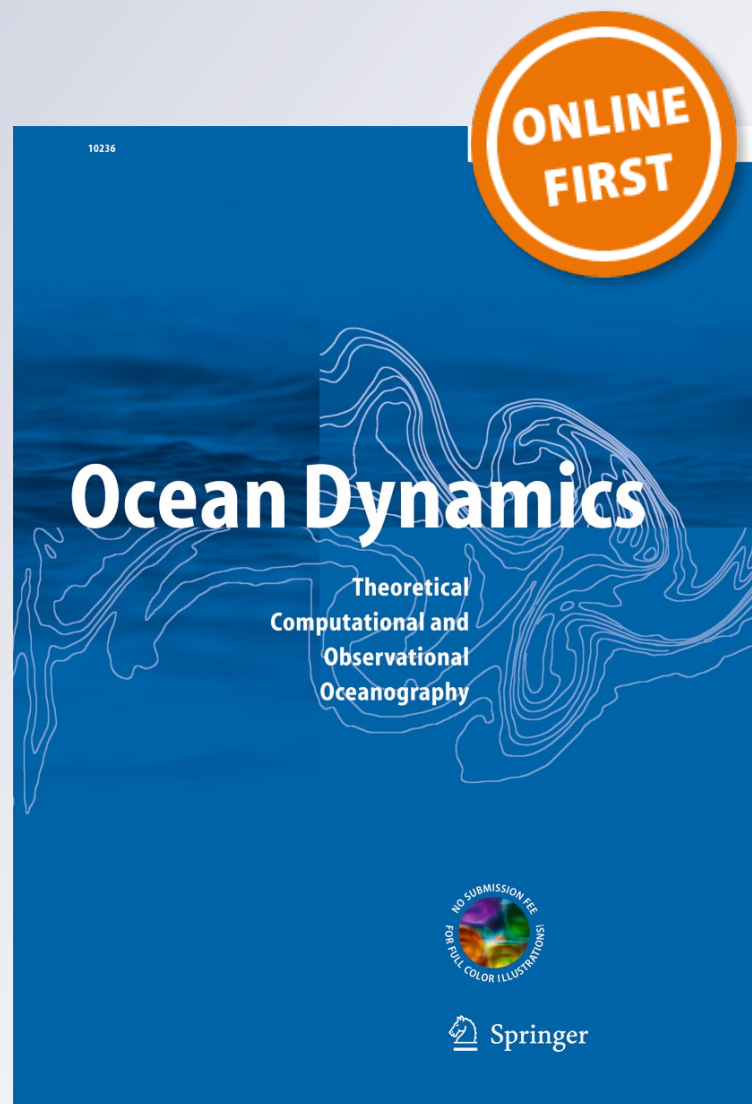ONLINE FIRST

Springer

Numerical modelling of morphodynamics—Vilaine Estuary

**Hans Jacob Vested · Caroline Tessier ·
Bo Brahtz Christensen · Evelyne Goubert**

Abstract The main objective of this paper is to develop a method to simulate long-term morphodynamics of estuaries dominated by fine sediments, which are subject to both tidal flow and meteorologically induced variations in freshwater run-off and wave conditions. The method is tested on the Vilaine Estuary located in South Brittany, France. The estuary is subject to a meso–macrotidal regime. The semi-diurnal tidal range varies from around 2.5 to 5 m at neap and spring, respectively. The freshwater input is controlled by a dam located approximately 8 km from the mouth of the estuary. Sediments are characterised as mostly fines, but more sandy areas are also found. The morphology of the estuary is highly influenced by the dam. It is very dynamic and changes in a complicated manner with the run-off from the dam, the tide and the wave forcing at the mouth of the estuary. Extensive hydrodynamic and sediment field data have been collected in the past and provide a solid scientific basis for studying the estuary. Based on a conceptual understanding of the morphodynamics, a numerical morphological model with coupled hydrodynamic, surface wave and sediment transport models is formulated. The numerical models are calibrated to reproduce sediment concentrations, tidal flat altimetry and overall sediment fluxes. Scaling factors are applied to a reference year to form quasi-realistic hydrodynamic forcing and river run-off, which allow for the simulations to be extended to other years. The simulation results are compared with observed bathymetric changes in the estuary during the period 1998–2005. The models and scaling factors are applied to predict the morphological development over a time scale of up to 10 years. The influence of the initial conditions and the sequence of external hydrodynamic forcing, with respect to the morphodynamic response of the estuary, are discussed.

Responsible Editor: Han Winterwerp

This article is part of the Topical Collection on the *11th International Conference on Cohesive Sediment Transport*

H. J. Vested (✉) · B. B. Christensen
DHI, Agern Allé 5,
DK 2970 Hørsholm, Denmark
e-mail: hjv@dhigroup.com

C. Tessier
DHI, 2/4 rue Edouard Nignon,
CS 47202, 44372
Nantes Cedex 3, France

E. Goubert
GMGL, Université de Bretagne Sud,
LDO UMR 6538,
56017 Vannes, France
e-mail: evelyne.goubert@univ-ubs.fr

1 Introduction

There is an increasing demand for the prediction of long-term morphology of estuaries for engineering and environmental management purposes. Numerical modelling of long-term morphodynamic behaviour of estuaries is extremely complicated as the hydrodynamic and sediment transport processes cover time scales ranging from seconds to years. A process-based long-term simulation with integration in time of numerical models requires long computation times, which in practise limit the predictions. Different techniques have been developed to reduce the computational burden, i.e. the selection of representative forcing or processes and morphological speed up factors (Roelvink and Reniers 2012). Major advances have

been made in morphodynamic simulations of sand-dominated estuaries on time scales of several decades; see for example Hibma (2004). For tidal-dominated, sandy and geometrically simple estuaries, Latteux (1995) developed the concept of a morphological tide, which can be applied to predict the long-term morphology.

In contrast to sand-dominated estuaries, there are fewer examples of morphodynamic simulations of mud-dominated estuaries. Waeles (2005) simulated the morphology of the Seine Estuary, taking into account sand and mud mixtures, for two 1-year periods with real historical forcing. A similar approach was applied by Lumborg and Pejrup (2005), who also applied real historical wind and wave forcing to model cohesive sediment transport in a Wadden Sea tidal lagoon, and who used the model results to establish the annual sediment exchange with the North Sea. van Ledden et al. (2006) modelled the sand–mud morphodynamics in the Friesche Zeegat for the period from 1970–1994. Focus was on the sand–mud segregation. The hydrodynamic forcing was synthesised to tidal flow and average wave conditions.

For cohesive sediments, the selection of representative forcing and the application of morphological speed up factors similar to sand transport are complicated by the seabed processes, such as consolidation, which strengthens the resistance to erosion with time. In many estuaries, the morphodynamics are impacted by climatic variations in run-off events and wave conditions on both an intra-annual and an inter-annual scale. The question of chronology may become decisive for the morphology.

The subject of this paper is to test a methodology to simulate the morphodynamic behaviour of a mud-dominated estuary. The time scale is up to 10 years. The methodology is based on applying a combined hydrodynamic, wave and sediment transport morphological model for fine sediments, taking into account layering of the sea bed. The hydrodynamic forcing is defined by real historical forcing data for a year with a representative chronology of events of river run-off, storm waves and tide. This year is used as a reference year, which is scaled to represent years with other combinations of waves and run-off conditions.

The methodology is applied to the mud-dominated Vilaine Estuary in France. It is tested to see whether it can reproduce the observed inter-annual morphological changes in response to wave forcing and river run-off. The applicability of the methodology is discussed both with respect to the Vilaine Estuary and in general.

2 The Vilaine Estuary

The Vilaine is a 220-km-long river. It drains an area of about 10,000 km^2 and enters the sea in the Bay of Vilaine, see Fig. 1.

This bay is separated from the Atlantic Ocean by islands and a peninsula, which provides some protection from westerly waves. The Vilaine Estuary is a meso–macrotidal estuary with a tidal range of 2.5 to 5 m at neap and spring, respectively. The progression of the tide and the freshwater run-off is controlled by the Arzal Dam, which is located approximately 8 km from the mouth of the estuary. During the dry period (August–September), the average daily flow released from the freshwater reservoir upstream the dam can be less than 5 m^3/s, and the tidal currents can be measured as far as to the dam. During flood periods with high river run-off (from the end of December to March), hourly release flow rates can reach 1,400 m^3/s, suppressing the tidal currents and flushing the estuary. The typical daily average of low and high river run-off is about 30 and 360 m^3/s, respectively. The yearly average discharge is 70 m^3/s.

Towards the east, the estuary is channelized in a meander, which becomes straighter as the estuary opens towards the Bay of Vilaine with large tidal flats at the mouth. In general, the estuary is divided into three parts (see also Fig. 1): (1) an internal channelized flow area dominated by the tide and the release flow from the dam, (2) an intermediate area with extensive tidal flats exposed to waves and tidal flow and to a lesser degree the release flow and (3) the mouth or external estuary, which is governed by wave forcing and tidal flow.

2.1 Morphodynamics processes of Vilaine Estuary

Prior to the construction of the dam, the sediment was resuspended and deposited over a distance of 50 km upstream of the mouth. Following the construction of the dam in 1970, the internal estuary silted up heavily during a period of 10–15 years. The dam stopped the sediment load from the upstream river and reduced the tidal volume significantly. As a result, the flushing and currents decreased, thus favouring deposition of sediment imported from the Bay of Vilaine. In addition, the tide changed from a progressive to a reflective tidal wave with an anti-node point in front of the dam resulting in reduced currents, which otherwise facilitated the siltation. The occasional strong release of freshwater from the dam scours a channel, which defines the flow in the internal part of the estuary. The sediment downstream of the dam is predominantly cohesive with an increasing content of fine sand and silt in the external estuary.

Two large field campaigns designed to support the modelling were undertaken in the Vilaine within the period March 2007–April 2008. The data collected were ADCP measured currents, waves, temperature, salinity, and turbidity in fixed positions, as well as sediment samples, settling velocity and altimetry at a tidal flat (Goubert et al. 2010). Furthermore, a time series of several months of sediment concentrations was collected using a MAREL Buoy in October–November 2006.
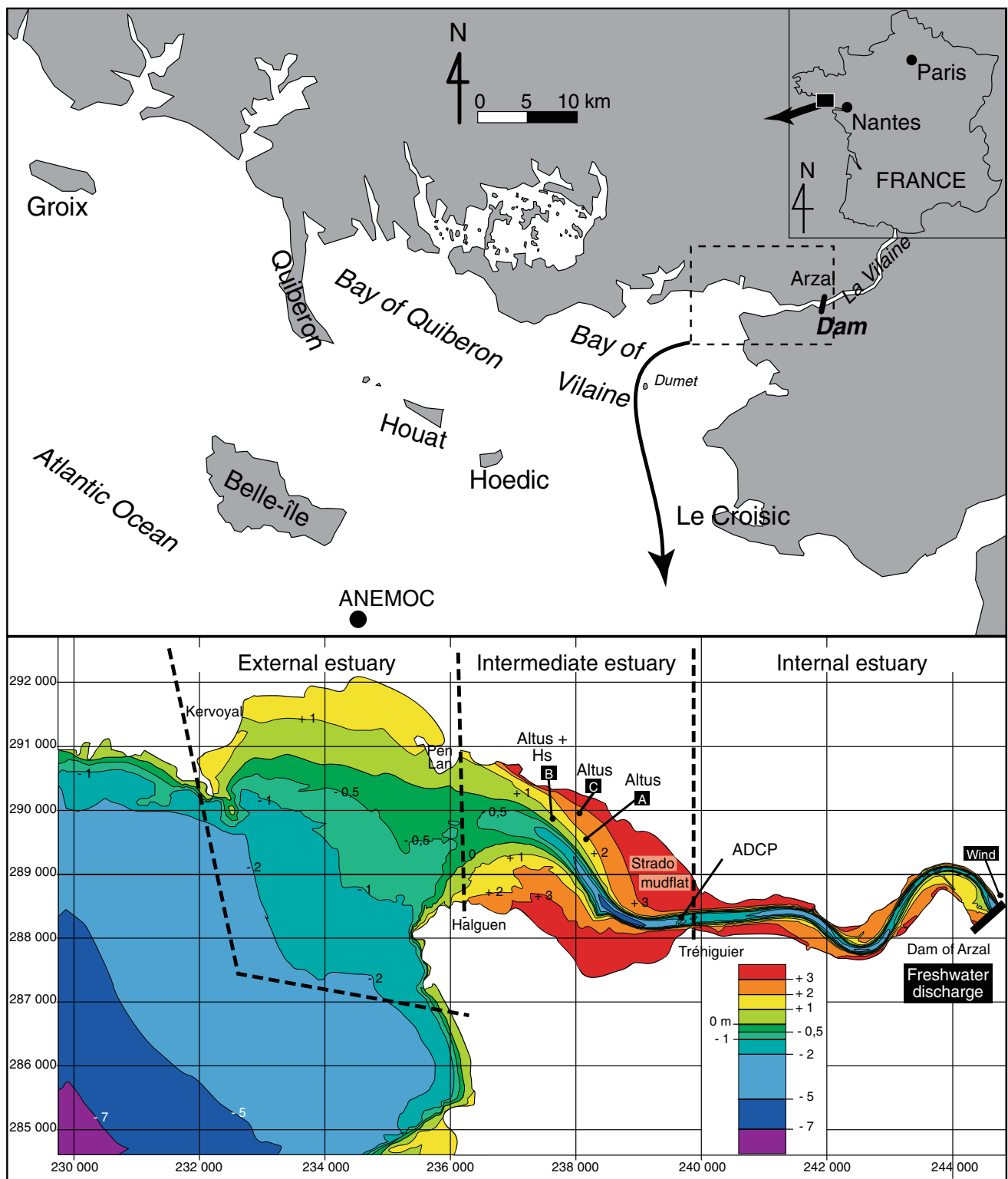
Fig. 1 The Vilaine Estuary. The map shows key locations, bathymetry of 2007 and position of the measurement stations. Reference level is chart datum

The data show that sediment concentrations vary with the tide, freshwater runoff and wave conditions. The concentrations can be very low during hydrodynamically calm periods. During periods with stronger currents, the concentration can be up to the order of 1,000 mg/l, see Fig. 9, which shows the measured concentration at Tréhiguier.

On the basis of historical bathymetric surveys carried out up to 2003, Goubert and Menier (2005) computed the siltation rates and sediment fluxes between the internal, intermediate and external estuary. They found that, during the period 1992–2003, the bathymetry of the estuary had reached a dynamic equilibrium. Due to variations in the import and export of sediment between the different parts of the estuary, the bathymetry could deviate from its equilibrium. Their analysis showed that a year with high river run-off resulted in an export of sediment from the internal estuary, while a year with low river run-off resulted in an import to the internal estuary. However, no clear correlation was found between run-off and the deposition–erosion pattern.

The bathymetry of the estuary has been surveyed every 2 years since 2001, and differential biennial maps have been determined (Goubert et al. 2010). Through inspection of these differential biennial maps, two situations have been identified, which synthesise the morphodynamics of the Vilaine Estuary. These situations are illustrated in Fig. 2, which shows the run-off from the dam and biennial differential bathymetric maps. Situation 1 is exemplified by the period from September 2003–September 2005, which had a lower river run-off. The differential bathymetry map shows that erosion is found in the external estuary simultaneously with deposition in the internal estuary. Situation 2 is illustrated by the period from September 2005–September 2007, which is characterised by a strong river run-off. During the winter sediment from the internal part is transported to the external estuary, where it can be observed several months after the run-off events.

2.2 A conceptual morphodynamic model

A conceptual morphodynamic model is formulated as follows: Erosion and deposition and the distribution of sediment between the three compartments of the estuary and the Bay of Vilaine are the result of the combined action of surface waves, dam discharge and tide. In the external estuary, sediment is brought in suspension by surface waves during storms. High dam release flows erode the internal part of the estuary and carry sediment towards the intermediate and external parts. The sediment load from the dam run-off is negligible. While weather-induced events occur only occasionally, the effect of tide is twice a day on a regular spring neap cycle. During low freshwater discharge, sediment from the external and intermediate parts is transported upstream by the tide. In order to further conceptualise the morphodynamic behaviour, four morphodynamic events have been identified as shown in Table 1: (A) tidal wave-dominated events characterised by strong waves in the external part of the estuary in combination with spring tide and low freshwater discharge. The strong waves and tidal currents resuspend sediments in the open and intermediate part. As the discharge is low, there is a net

tidal induced import of sediment to the internal estuary. (B) Tidal-dominated events similar to A but with small waves, and consequently, there is less re-suspension in the external part and therefore a smaller import to the internal part. (C) Wave-dominated events with smaller tidal forcing resulting in a lower import. These events are all capable of importing marine sediment, which is the only source of sediment to the estuary after the closure of the dam. (D) Discharge-dominated events when the river run-off is high, in combination with strong or weak waves, neap or spring tide. Discharge-dominated events result in an export of sediment from the internal estuary towards the mouth and open part of the estuary. It is important to note that if a strong run-off occurs simultaneously with strong waves, the potential for a permanent deposition in the open part is less. During dry and calm periods, the hydrodynamic forcing is low and sediment suspensions small with very small morphodynamic changes. During situations with high run-off, the estuary changes from being flood-dominated to ebb-dominated.

It is the balance between the event driven imports and exports of sediment and the occurrences and durations of these events that determines the morphodynamics. This becomes a very delicate balance due to the importance of the timing of events. A significant change in the bathymetry is observed, but overall the estuary is in a dynamic equilibrium.

3 Model set-up

The hydrodynamics, surface waves and sediment transport are modelled using MIKE 21 FM (Flexible Mesh) with a coupling of the hydrodynamic (DHI 2009a), spectral surface waves (Sørensen et al. 2004) and sediment transport modules (Petersen and Vested 2002; Lumborg and Pejrup 2005). These modules simulate the bed evolution in 2D due to depth-averaged tidal flow, wind-induced flow, dam release flow and the effect of the combined current–wave bed shear stresses. The 3D processes, such as helical flow, salinity stratification and density driven flow, are not included. A salt water wedge is observed in the estuary during high freshwater run-off, but it was decided to apply the 2D model to simulate the morphological evolution for the long-term simulations (1 to 10 years) and accept that the uncertainty due to the lack of inclusion of 3D effects is covered in the general calibration parameters.

Both a regional and a local hydrodynamical model have been set up (Fig. 3). The local model covers an area from the dam to the seawards limits of the Bay of Vilaine. The computational mesh is defined by triangles and quadrangles. The mesh size is about 1,000 m for triangles in the open sea and decreases to 100 by 20 m for quadrangles in the interior of the estuary. The open boundary conditions for the local model are the water levels, simulated by the larger regional
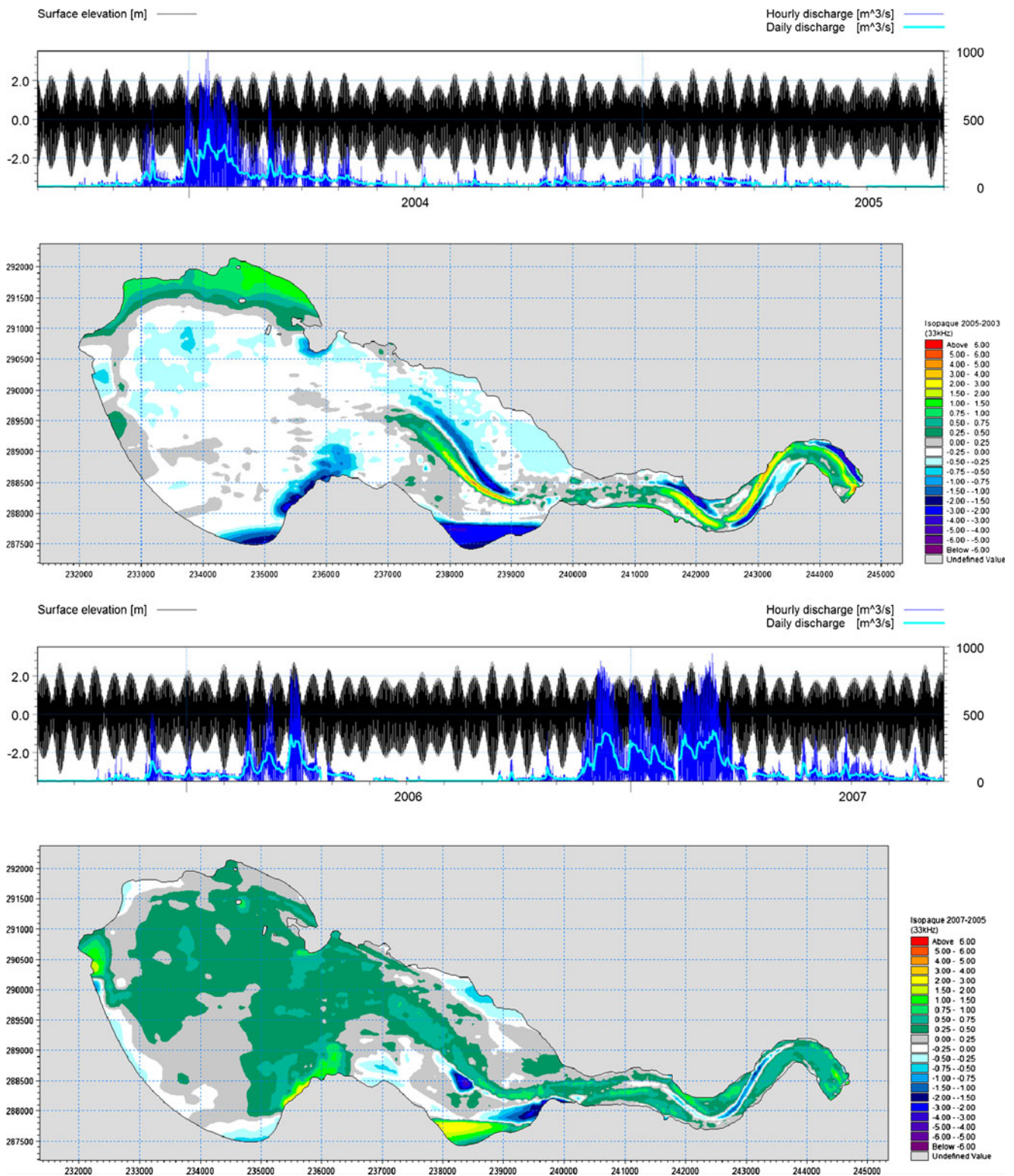
Fig. 2 The upper panel shows the dam release flow (hourly and daily values) and the tidal variation from September 2003–September 2005. The map below this shows the differential bathymetry for the same period. The lower panel shows the same information but from September 2005–September 2007

model (Fig. 3), which is forced by the astronomical tide, along its open boundaries, defined by tidal constituents from the French Maritime Organisation (SHOM). In addition, the local model is forced by the wind measured at Arzal at the

Table 1 Schematisation of morphodynamic events

Type		Tide (T)	Waves (W)	Discharge (Q)	Morphodynamic impact
A	T/W dominated	Spring	Strong	Small	Suspension open sea, strong import to estuary
B	T dominated	Spring	Weak	Small	Small import to estuary
C	W dominated	Neap	Strong	Small	Small import to estuary
D	Q dominated	Spring/Neap	Strong/Weak	Strong	Suspension open sea, strong export from estuary

dam. The upstream boundary condition of the local model is the release flow or run-off from the dam. Hourly discharge values from the actual recordings are applied.

Wind-generated surface waves from a larger offshore spectral wave model of the English Channel and the French Atlantic coast are transferred through the regional model to the local model. The local wave model applies the same computational mesh as the hydrodynamic model.

A sediment transport model is set up for the local model area. The model is dynamically coupled with the hydrodynamic model and the wave model in order to update the bathymetry and prepare morphological simulations.

The simulation period is from March 2007 to April 2008 during which period field data were collected for calibration. The time step for the hydrodynamic and sediment transport simulation is variable and depends on the stability criteria for the explicit numerical schemes. The maximum time step was set to 60 s. The time step for the wave simulation was 900 s for a quasi-stationary solution scheme.

Firstly, a wave simulation is made with a fixed bed. The water depths for the wave simulation varied in time with the surface elevations defined by the astronomical tide over the model domain. Secondly, a dynamically coupled hydrodynamic and sediment transport simulation is made. The bed is updated with the time step of 60 s. The bed shear stresses for

the sediment transport depend on both the currents and the wave conditions, which are determined from the wave simulation with a fixed bed. The wave data are input each 900 s. The procedure is schematized in Fig. 11.

The Vilaine Estuary is characterised by both cohesive sediments and fine sand/silt. The sediment processes are sketched in Fig. 4. An overview of the model equations are given in Fig. 5. The sediment transport model is based on a solution of the advection–dispersion equation for suspended sediments, with the seabed–water interface included as source and sink terms. The open boundary towards the Bay of Vilaine is zero influx of sediment. Sensitivity tests with a small ocean background concentration showed no impact on the results. The open boundary condition at the dam is also zero influx, as measurements show a negligible content of sediment in the run-off.

The seabed–water interface follows the classical Krone formulation for deposition and the Partheniades–Ariathurai erosion law.

$$S_d = wc_b \left(1 - \frac{\tau_b}{\tau_{cd}} \right), \text{ when } \tau_b < \tau_{cd}$$
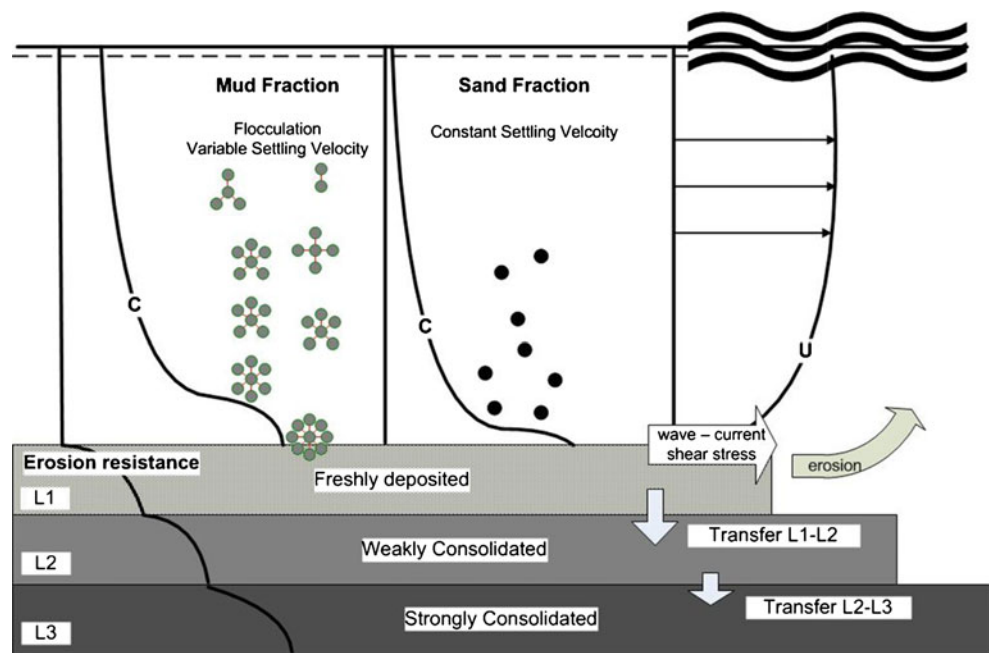
$$S_e = E_0 \left(\frac{\tau_b}{\tau_{ce}} - 1 \right), \text{ when } \tau_b < \tau_{ce}$$

Fig. 3 Results from regional models of tidal flow and spectral waves are used as boundary conditions for the local model of the Vilaine estuary
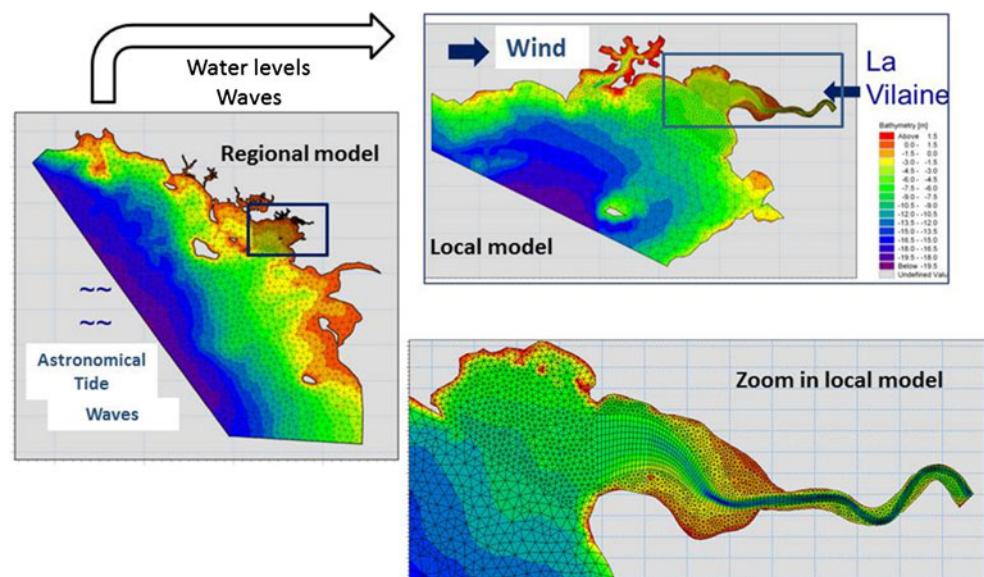
Fig. 4 Schematisation of the sediment processes with a mud and a sand fraction in the water column

w is the settling velocity, c_b the near bed sediment concentration calculated according to Teeter (1986), τ_b the bed shear stress due to skin friction, τ_{cd} the critical shear stress for deposition, E_0 the erosion rate and τ_{ce} the critical shear stress for erosion.

Both currents and surface waves contribute to the bed shear stress. The resulting bed shear stress τ_b is computed using a combination of bed shear stresses from waves and currents. The model applies the Soulsby et al. (1993) parameterisation of the maximum shear stress from the wave–current boundary layer theory of Fredsoe (1984).

In order to account for both fine sand/silt and cohesive sediments, two fractions are simulated, defined by the settling velocity. The fine sand/silt is assumed to have a constant settling velocity of 8 mm/s. The cohesive sediment flocculates, and the settling velocity increases with increasing cohesive sediment concentration c according to an equation of the form (see for example Whitehouse et al. 2000):

$$w = kc^\gamma$$

This equation is applied; however, the concentration is made dimensionless with the mineral grain density $\rho_s = 2650$ kg/m^3, in order to make the exponent independent of unity. The equation is applied for a sediment suspension between 0.01 and 10 kg/m^3 and reads

$$w = w_0 \left(\frac{c}{\rho_s}\right)^\gamma = 0.265 \left(\frac{c}{2,650}\right)^{0.6}, \text{ when } 0.01 < c < 10 kg/m^3$$

The equation gives a variable settling velocity of 0.15–9 mm/s for a sediment suspension between 0.01 and 10 kg/m^3. This is in the same range as in situ Owen Tube measurements of 0.05 to 7 mm/s collected during March 2007.

The bed is modelled by three sediment layers: (1) a surface layer with a dry density of 200 kg/m^3 representing soft mud, (2) a second partially consolidated layer with a dry density of 500 kg/m^3 and (3) a consolidated layer with a dry density of 800 kg/m^3, which only erodes during floods and storms. The effect of the consolidation is parameterised, by a transition of mass from one layer to the layer below, similar to Teisson (1991). The sediment settles to the first layer, and the transition from one layer to the next is described by a mass transfer rate (kilogrammes per square metre per second). This transition represents the motions of the boundaries between the three layers. The transfer rate is 10^{-3} kg m^{-2} s^{-1} from the first to the second layer and 10^{-6} kg m^{-2} s^{-1} from the second to the third layer.

An overview of the sediment transport equations and their relationships is presented in Fig. 5, modified from Lumborg and Pejrup (2005).

The initial conditions for the sediment model are defined by the thickness of the bed layers and the spatial composition of mud and sand. Areas, mostly along the coast where the seabed is rock, are initially defined to have no sediment. The spatial distribution of thickness of bed layers 1 and 2 is further initialised by running the model two times for the simulation period March 2007 to March 2008 before starting the proper simulations. This approach was necessary in order to reduce a strong impact of the initial conditions on the results.

Grain size analyses of sediment bed samples have shown that typical grain sizes are around 10 and 90 μm, and the mud content is 60 to 80 %.
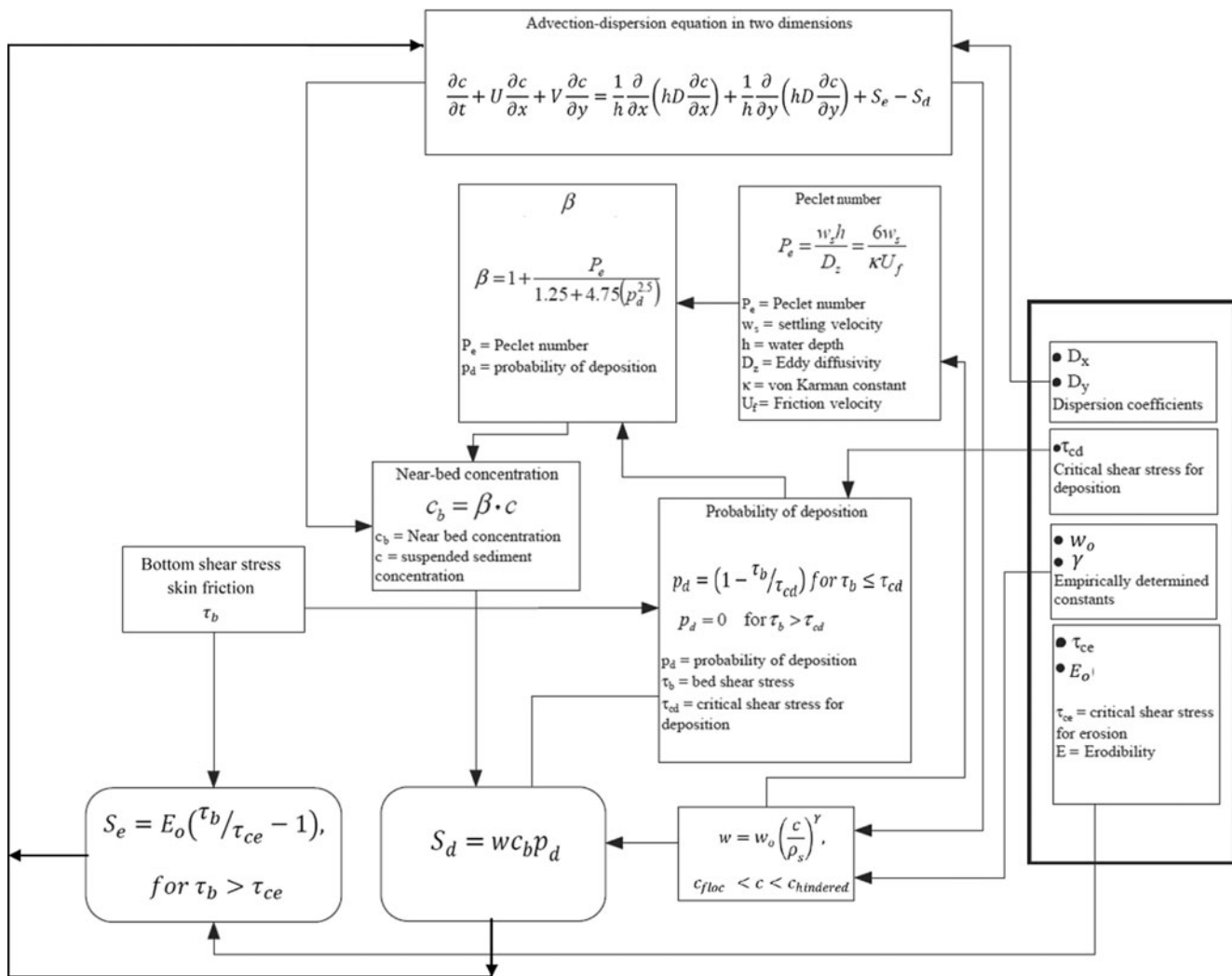
Fig. 5 Overview of equations, modified from Lumborg and Pejrup (2005)

It is assumed that the first layer of the bed has a dry density of 200 kg/m³. However, in reality, the dry density of the upper bed layer can be lower than the prescribed value and will vary in both time and space. In order to guide the calibration, the expected range of critical shear stresses for erosion of sand–mud sediments has been evaluated. The conceptual relationship in Le Hir et al. (2011) has been applied for the evaluation. This is outlined in Fig. 6.The critical shear stresses for erosion can be estimated by the relation of Mitchener et al. (1996) based on a range of mixed beds, consolidated beds and blended sand–mud beds.

$$\tau_{\text{ce}} = E3(\rho_b - 1{,}000)^{E4}$$

where $E3 = 0.015$ and $E4 = 0.73$ are dimensional coefficients (SI units) and ρ_b is the bulk bed density in kilogrammes per cubic meter. Increasing the bed density results in an increase of bed resistance. With a sand grain size of $d_{50} = 0.10$ mm, the Shields criteria can be applied to define a critical shear

stress for pure sand. It is assumed that there is a maximum resistance for sand with a 30 % mud content of about five times the resistance for pure sand Whitehouse et al. (2000), and with a mud content of 70 %, it behaves as pure cohesive sediment. This variation is illustrated in Fig. 6.

Figure 6 indicates that for a mud content of 60–80 %, one can expect critical shear stresses in the range of 0.2 to 0.5 Pa.

It requires a significant effort to calibrate the sediment transport model with its many empirical parameters. Based on the observations of settling velocity, and the estimates of critical shear stresses for erosion relative to bed density, the expected range for these values could be estimated to guide the calibration. The calibration thus became an effort to apply these ranges, and determine erosion and transition rates between the bed layers, in order to be able to reproduce the observed concentration of suspended sediments. Simultaneously, realistic sediment fluxes between the different estuary sections should be reproduced and morphodynamic stability over tidal flats

Fig. 6 Conceptual variation of the critical shear stress in pascals for the erosion of sand and mud mixtures with varying dry bed density. Grain size of sand is d_{50}=0.1 mm
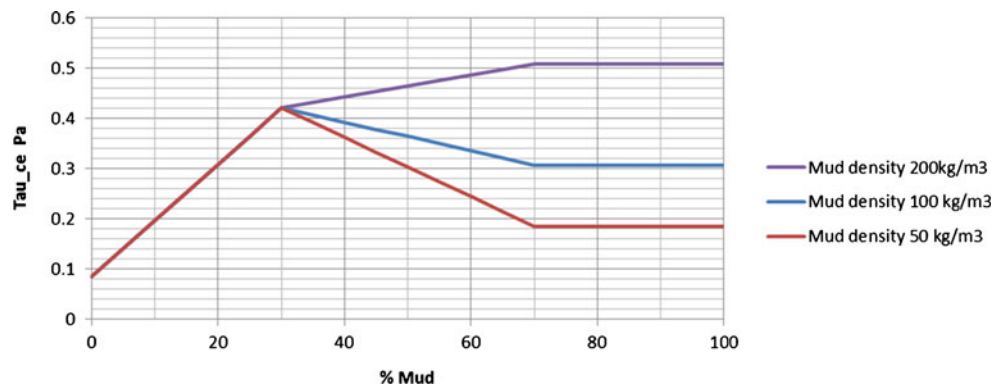
maintained. To achieve this, it was realised that a spatial distribution of the critical shear stress for erosion was required in order to describe the heterogeneous character of the sediment behaviour. The definition of the spatial distribution was guided by the information of sand and mud contents as well as a distinction between deeper water and the inter-tidal flats. Figure 7 shows the spatial distribution of the critical shear stress for layer 2. The distribution is defined by the four values separated by slashes as shown in Table 2 for layers 1 and 2. For layer 2 as example, τ_{ce} is defined by the values 0.85, 0.7, 0.6 and 0.5 Pa. The higher values are applied in the external estuary and the deeper channel, while the lower values are applied in the internal part and over the mudflats. For layer 3, no spatial distribution was applied. It should be mentioned that with the applied settings, layer 1 is less significant for the results. It either rapidly erodes or its material consolidates and is transferred to layer 2.

Table 2, third column, gives the range of values of τ_{ce} one would expect according to Fig. 6. It is seen that these values are in accordance with the range of calibrated values given in the fourth column of Table 2. Table 2 also gives the erosion coefficient E_0, which is almost constant for the three layers.

The necessity of applying relatively high values for τ_{ce} in the mouth of the estuary and tidal channel may be explained by the so-called drag reduction. Suspended cohesive sediments may cause damping of the turbulent fluctuations in flowing water and may alter the apparent bed roughness, thus leading to a drag reduction Toorman et al. (2002). In Winterwerp and Kesteren (2004), the impact of high-concentration mud suspensions (0.1 g/l to several grammes per litre) and their effect on the hydrodynamics are thoroughly discussed. The sediment–fluid interactions can lead to drag reduction or saturation of the water column. Similar to what is reported in Winterwerp and Kesteren (2004), for estuaries with high concentration mud suspensions, it was found that a relatively low friction was required to calibrate the hydrodynamic model (Manning number $n=$ 0.0143 s/m$^{1/3}$) for the Vilaine Estuary indicating that this phenomena may be present. The model does not include the effect of drag reduction. This would require a coupling of the hydrodynamic friction and the bed shear stress calculation in the sediment transport model. The effect of drag reduction was therefore compensated for by a higher value of τ_{ce}.
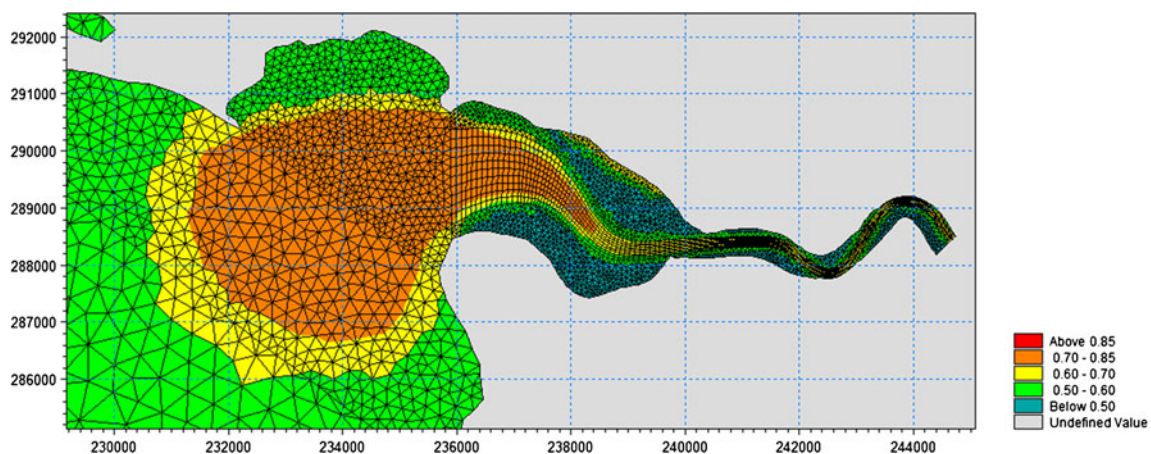
Fig 7 Horizontal distribution of τ_{ce} of layer 2. The spatial distribution is defined by the values 0.85/0.7/0.6/0.5 Pa

Table 2 Erosion parameters for the three bed sediment layers, comparison between expected literature and calibrated values

The values separated by slashes correspond to the values applied in the spatial distribution

	Dry density range [kg/m^3]	τ_{ce} [Pa] Figure 6	τ_{ce} [Pa] calibration	E_0 [kg/m^2/s] calibration
Layer 1	50–200	0.2–0.5	0.425/0.35/0.3/0.25	5.0 10^{-4}
Layer 2	200–500	0.5–1.0	0.85/0.7/0.6/0.5	4.5 10^{-4}
Layer 3	500–800	1.4–1.4	1	4.5 10^{-4}

A critical shear stress for deposition map, with a configuration similar to Fig. 7, was also prepared. The applied values were 0.72, 0.63 and 0.54 Pa. The low values were applied over the tidal flats. It is noted that τ_{cd} was larger than τ_{ce} for layer 1. This was necessary to reproduce the observed sedimentation rates.

4 Simulation methodology and calibration

The simulation methodology builds on the assumption that the estuary is in a dynamic morphological equilibrium over a longer period in time with fluctuations around this equilibrium, cf. Section 2.

Firstly, it is shown that the period March 2007–March 2008 is representative for the occurrence of typical morphodynamic events and can be applied as a reference year. Secondly, it is shown that the model set-up described in Section 3 can reproduce the short-term measurements available in the period March 2007–March 2008. Thirdly, the methodology for scaling the reference year for other combinations of forcing is presented. Finally, it is shown that the reference year scaled to historical forcing can be applied to simulate the trends in morphodynamic evolution over a 7-year period from 1998 to 2005.

4.1 Definition of a reference year March 2007–March 2008

Figure 8 shows significant wave heights at a point in the Bay of Vilaine, tidal variations at the dam, hourly dam release flow rates and wind speed at the dam for the period March 2007–March 2008. The typical morphodynamic events of type A, B, C and D defined in Table 1, governing the exchange of sediment between the internal and external estuary, can be identified. In March 2007, there was a very high run-off, as well as high waves and a spring tide (type D) at the same time. From May to August, wave conditions are frequently high in combination with a lower but not insignificant run-off (types C and A). Around October, there is a situation with small waves combined with low run-off (type B). In December, higher waves occur while the run-off is not too high (type C). In the winter months of January, February 2008 high waves and strong run-off occur (type D).

Thus, as the period March 2007 to March 2008 contains a combination of all the typical morphodynamic events, it will be applied as a reference year, which can be scaled to represent other combinations of the strength of waves/winds and dam release flow.

4.2 Short-term calibration results for the period 2007–2008

The short-term calibration is based on the period from March 2007 to April 2008 (13 months). Within this period, field data were collected in March 2007, and Altus measurements (Goubert et al. 2010) were available from autumn 2007 to spring 2008.

During a 15-day period from 14 March to 29 March 2007, currents, water levels and suspended sediment concentrations were measured at three fixed stations in the estuary. The conditions in the estuary during this period are illustrated in Fig. 9. Spring tide occurred around 20–21 March. The hourly discharge from the dam release flow was 500–700 m^3/s. It is worth noting that water is always released during the falling tide. A NW–N storm took place around 18 to 20 March with a significant wave height of 1.5 m in the Bay of Vilaine and 0.4 m over the northern tidal flat at the mouth of the estuary (Strado mudflat).

The calibration is based on a 13-month simulation with the wave model and the coupled hydrodynamic and sediment transport models for the period of March 2007 to April 2008.

The wave and hydrodynamic models were calibrated to a high degree of accuracy to reproduce the measured waves, water levels and currents at the fixed stations in the estuary. This was required as the basis for modelling of the sediment conditions. An example of the comparison of simulated and measured currents and water levels is shown in Fig. 9. Due to the large tidal variations, the wave conditions over the shallow areas depend on the actual tide. This is illustrated in the upper panel of Fig. 9, which shows the simulated wave height in the mouth of the estuary together with the simulated surface elevation. During the storm on 18–20 March 2007, the wave heights are smaller at low tide and increase at high tide, see Fig. 9 upper panel. A detailed description of the analysis of hydrodynamic conditions and the calibration of the model is presented in DHI (2009b).

Fig. 8 Waves (H_s), tidal elevations, dam discharge and wind speed at the dam for the reference year March 2007– March 2008 applied to force the model. It contains the typical morphodynamic events (**a**–**d**)
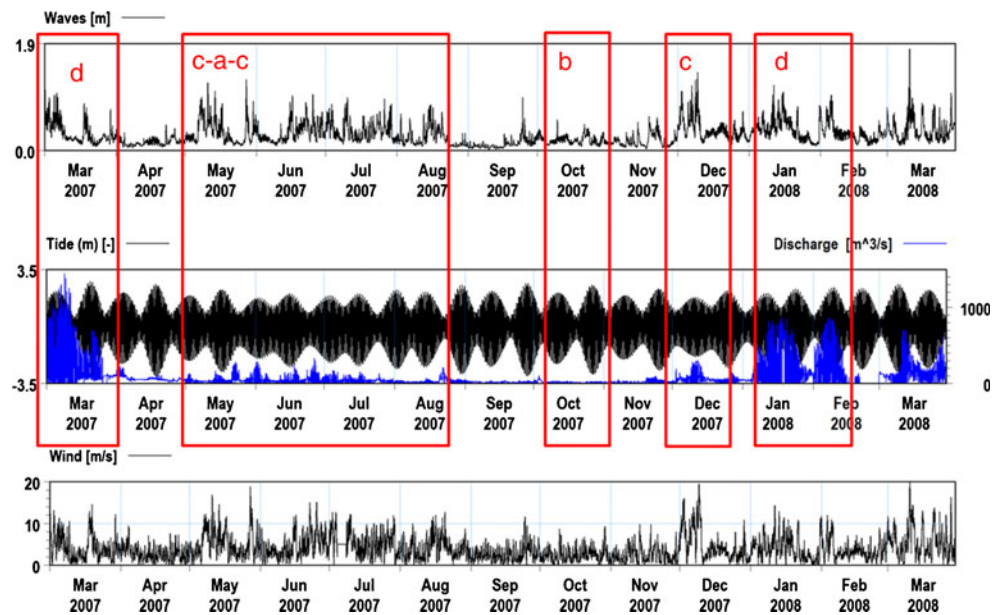
Fig. 9 Hydrodynamic and sediment conditions from 17–24 March 2007. Comparison between measured and simulated water levels, depth averaged current speeds (m/s) and sediment concentrations (grammes per litre) at Tréhiguier (see Fig. 1). Sediment concentration measurements are taken at the surface (*black*) and at the bottom (*green*)
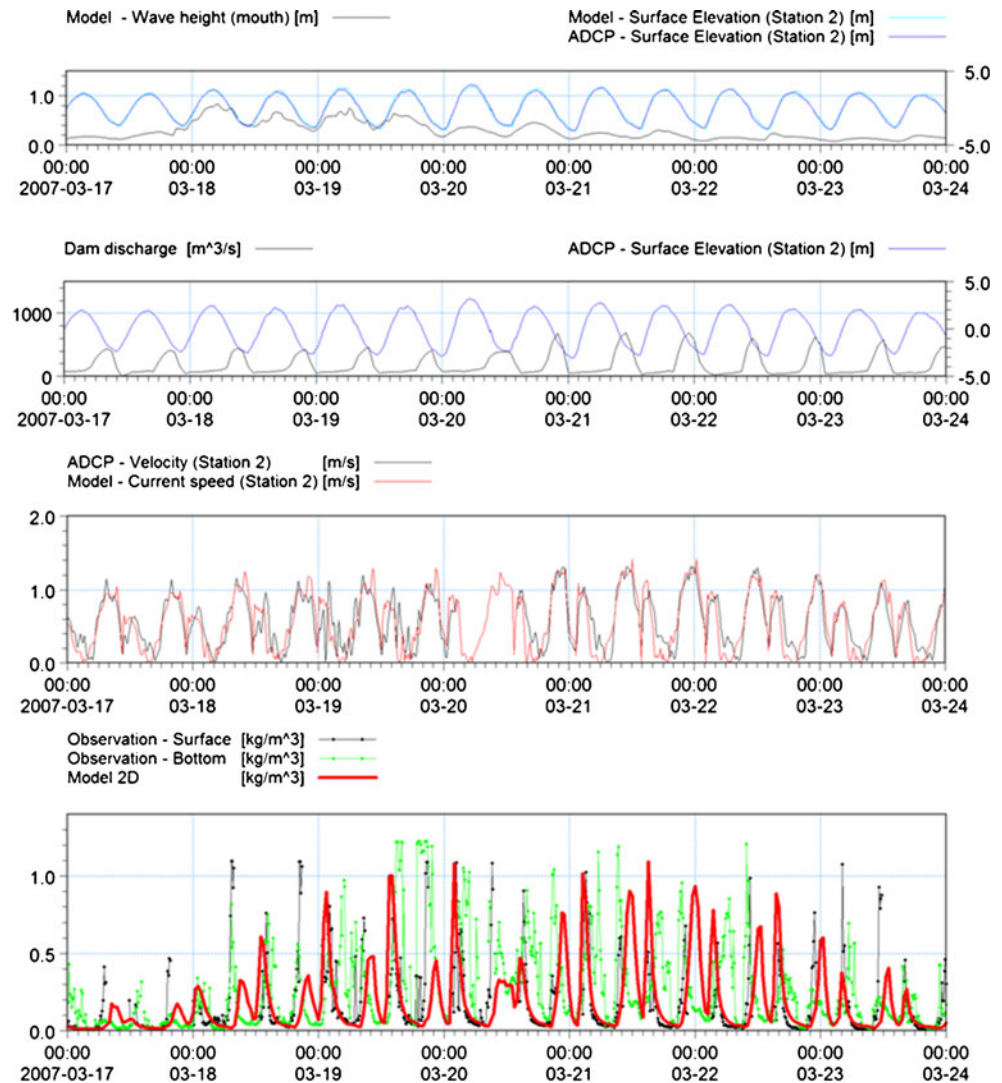
In general, it is found that the measured sediment suspensions vary with the semi-diurnal tide, but an influence from waves is also observed. In the estuary channel close to Tréhiguier, the concentrations show a tidally influenced variation. Peak concentrations reach 1,000 mg/l for rising and falling tide around 19–22 March 2007, see Fig. 9. The elevated concentrations are likely linked to the storm, which sets in on 18 March and resuspends sediments in the external estuary. The storm thus increases the amount of mobile sediments, which can become subject to advection by the tidal currents. The model reproduces the observed variability with a shift in values from about 15 to 1,000 mg/l. It should be mentioned that a better comparison was obtained for this particular situation Tessier et al. (2012), with a slightly different calibration. However, when this calibration was applied for longer simulations covering several years, the results drifted.

With the objective to prepare morphological simulations, it is important to calibrate towards observed seabed evolutions. For this purpose the model was compared with altimetry measurements (Altus instrument, Jestin et al. 1998) for a 5-month period in three positions (A, B and C) at Strado mudflat, the tidal flat north of the channel entrance, see Fig. 10. The Altus shows erosion events induced by storms from December 2007 and the accretion on the bank of mudflat (B) during the high river discharge period (January–February 2008). During the second half of February 2008 and the beginning of March, there was a continuous increase in seabed level at the most seaward measurement position B. This is likely caused by reworking of sediment deposits from the floods due to easterly waves and/or secondary tidal currents. Secondary currents may be generated by helical flow or axial convergence/divergence flow in this relative narrow part of the estuary. Small-scale

sea bed waves or ripples have also been observed at the bank, which complicates the interpretation of the Altus point measurements. The model reproduces the evolution of the mudflat although with amplitudes slightly lower than those observed. During easterly winds, the model does not reproduce the observed behaviour of the bed elevation in points B and C. This could be due to a lack of model resolution. The model is not able to simulate the exchange of sediment across the northern mudflat or between both mudflats on either side of the channel, when small waves generated by easterly winds rework the mudflats.

Finally, in order to check the overall behaviour of the model, the accumulated simulated sediment fluxes at the end of the 12-month calibration simulation period were compared with observed sediment fluxes across estuary sections (Goubert and Menier 2005), see also Section 5.1 and Fig. 13.

A large number of calibration simulations had to be performed in order to determine the model parameters. The most important calibration parameter was τ_{ce} for the three sediment layers. The large range of bed shear stresses due to tidal flow, river run-off and surface waves both horizontally and over time made the results very sensitive to τ_{ce}. The second most important calibration parameter was the settling velocity. Initially, a constant settling velocity was applied, but the dependency of sediment concentration gave a better agreement with measured suspended sediment concentrations. The third important calibration parameter was the transition rates of mass between the bed layers needed in order to move deposited sediment to the more resistant bed layers and avoid immediate resuspension. As mentioned in Section 3, it was realised that a spatial distribution of τ_{ce} was necessary to describe the heterogeneous character of the sediment behaviour, and this distribution became part of the calibration. The more easily calibrated parameters were E_0 and τ_{cd}.
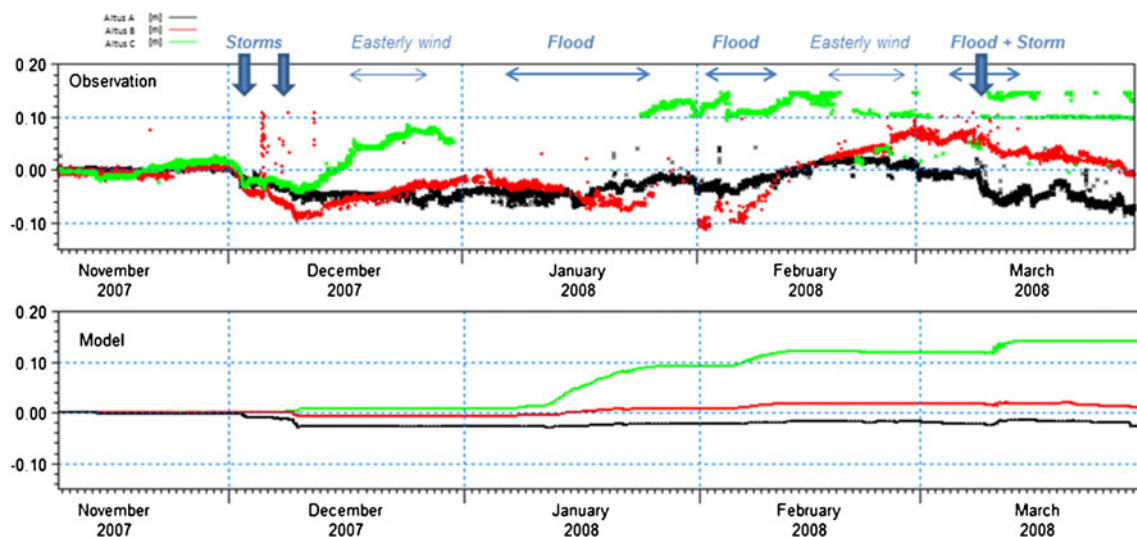
Fig 10 The evolution of seabed level (metres) (observed and modelled) at three Altus stations (A *black*, B *red* and C *green*) on Strado mudflat

4.3 Definition of forcing functions

The model has been calibrated to reproduce suspended sediment concentrations for short-term periods and trends in tidal flat altimetry measurements collected in March 2007–March 2008. The next step is to determine how the forcing functions, i.e. river run-off, waves and wind for this period, can be scaled to represent other years.

The release of water from the dam has been recorded daily since 1970 and hourly since 2003. The hourly values can be up to two times higher than the daily values and the sudden run-off induces a strong scouring of the internal estuary. Thus, the hourly values must be applied to force the model. The hourly run-off values have been analysed statistically for the period 2003–2008 and categorised into three classes: high, medium and low run-off. The occurrence of these events has then been established by using the daily records from 1970. This has been done by considering the percentage of time of a year (April to April) that the run-off exceeds a threshold of 200 m^3/s. This analysis shows that there is on average a year with high run-off every 6 years, and during the period from 1988 to 1992, there were five consecutive years with a low run-off.

A 23-year-long time series of offshore waves for the period 1979–2002 is available in the French wave data base ANEMOC. A point at a depth of 53 m (ANEMOC point n°1499), see Fig. 1, was applied to determine the long-term wave climate. In general, the waves come from the SW. Similar to the run-off, three classes have been defined: high, medium and low waves. In order to classify the years, the ratio of the percentage of the times per year that the wave height exceeds 2.5 m to the average for the 23 years was evaluated. The occurrence of medium waves corresponds to a ratio from 0.85–1.15. If the ratio is less than 0.85 or higher than 1.15, it is either considered as a year with low waves or high waves. The classification based on this analysis is presented in Table 3. No offshore wave data are available in the ANEMOC data base for 2003 up to the present. The wave forcing has for this period been estimated on the basis of the wind climate defined by the measured local wind at the dam. These years are indicated by brackets.

The joint probability of the occurrence of high, medium and low river run-off and wave forcing has been defined based on the classification in Table 3 for the years from 1976 to 2009, see Table 4. The number of occurrences of combinations of events has been counted for the 33 years of data for which data has been available. Table 4 shows, for example, that the probability of a year with high waves and river run-off is about 0.12 or about one in 10 years. Likewise, the probability of a year with low waves and river run-off is about 0.2, which on average corresponds to two in 10 years.

The events have been normalised to represent a period of 10 years. The possible number of combined events is listed in Table 4.

The next step is to determine how to scale the run-off, wave and wind forcing for the reference period April 2007–April 2008 in order to reproduce the high, medium and low events listed in Table 4. By scaling of the reference period, it is assumed that the intra-annual variation and sequence of forcing, i.e. tide, run-off and waves, is the same for all nine combinations of events in Table 4, but with different scaling factors. The hypothesis is that the reference period contains all the important morphodynamic events (types A, B, C and D) and it can be scaled to represent other years.

The scaling factors apply to the local hydrodynamic and wave model boundary conditions. Three scaling factors are required, one for the run-off from the dam, one for the wind speeds, which are applied over the local model area, and one for the wave heights that are specified along the open boundary for the wave model. The estimation of the scaling factors is based on an assessment of the annual energy input E of run-off, the wind and the waves.

A measure for the annual energy is calculated from the historical time series by considering the sum of the square of the run-off Q, the wind speed W_s and the waves H_s for the individual years. The scaling relative to the period April 2007–April 2008 is then derived from the expression:

$$f_x = \sqrt{\frac{E_{NX}}{E_{\text{refX}}}} = \sqrt{\frac{\int_{\text{April year N}}^{\text{April year N+1}} X^2 \mathrm{dt}}{\int_{\text{April 2007}}^{\text{April 2008}} X^2 \mathrm{dt}}}$$

where f_x is the scaling factor and X can be Q, W_s or H_s. The quadratic scaling puts more weight on the strong events.

The quadratic scaling of the wind speed corresponds to the force exerted by the wind on the sea surface, which is proportional to the square of the wind speed. The quadratic scaling of the wave heights, applied along the open boundary for the local wave model, is in accordance with the wave-induced bed shear stresses that scale with the square of the orbital wave velocity, which is proportional to the height of the waves.

The erosion due to river run-off scales through bed shear stresses with the velocity squared or the square of the discharge applied at the boundary at the dam.

The scaling factors for the run-off have been calculated for the years 1998 to 2009 and are listed in Table 5. Two sets of scaling values are shown, one based on daily values for the entire period, and one based on hourly values for the period 2003–2008. It is seen that the difference between the scaling factors based on hourly and daily values is small.

Simulation of the period from 1998 to 2005 revealed that application of the scaling factor for run-off (second and third column in Table 5) resulted in an exaggeration of the flushing from the internal estuary and an underestimation of the

Table 3 Classification of the years 1970–2009 based on run-off and wave conditions

Significant wave height	High run-off	Medium run-off	Low run-off
High waves	1993, 1994, 2000, 2002	1978, 1983, 1989, (2008), (2007)	1985
Medium waves	1981, 1987, 1998, (2006), (2009)	1982, 1984, 1999, 2001, (2003)	1986, 1991, 1992, 1997
Low waves		1979, (2004)	1980, 1988, 1990, 1991, 1995, 1996, (2005)
Waves uncertain (not considered)	1976	1971, 1974, 1977	1970, 1972, 1975

import of sediment during low flow. Accordingly, the scaling factor for river run-off was calibrated to make the model reproduce the behaviour observed in the bathymetric differential maps. These values are listed in Table 5, fourth column. The calibrated values are generally smaller by a factor of 2. This reduction in scaling factor is necessary because of (1) an intra-annual variability in the forcing from year to year, which cannot be scaled in a simple manner, (2) uncertainties related to sudden high frequency (less than tide) forcing by peak release flows from the dam, which scour the internal estuary channel (the limitation of the methodology to scale this effect) and (3) 3D effects not accounted for in the 2D model.

The quadratic scaling of the dam discharge gives more weight to stronger events. This may overestimate the export, due to advection, of sediment eroded from the internal estuary. The linear scaling factors have also been evaluated. It was found that the linear factors are not very different from the quadratic factors when no lower threshold value for run-off was applied.

The observed wind at Arzal, during the period 2003 to 2010, was also analysed to determine the scaling factors to be applied due to wind forcing. Only wind directions from westerly directions higher than 5 m/s have been taken into account. This analysis results in scaling factors of 0.8/0.9/1 for low, medium and high wind forcing events.

As the wave generation depends on the square of the wind speed, and in the absence of a long time series of waves for the Bay of Vilaine, the scaling factors for the waves were simply determined by computing the square of the factors for winds. This results in scaling factors of 0.7/0.8/1 for low, medium and high wave forcing events.

4.4 Morphodynamic simulation from 1998–2005

In order to evaluate whether the model forced by the scaled reference year can describe the erosion–deposition patterns over a period of several years, the morphodynamics have been simulated for the period 1998 to 2005 with the bathymetry from 1998 as the initial conditions.

The scaling factors are applied to scale the open boundary conditions for the reference year to represent the individual years. For example, low waves are determined by a simulation of the local wave model with the open boundary conditions for wave heigths multiplied by 0.7 and wind speeds reduced by a factor of 0.8.

The morphological update procedure is shown in Fig. 11. Each year of simulation continues with the bathymetry and sediment conditions (spatial mass and fractions) from the previously simulated year. During the simulations, the bathymetry is updated as a function of the thickness of the bed sediment layers, and this is fed back into the hydrodynamic equations. However, the bathymetry for the wave simulations is only updated prior to the following year's simulation. This is of course a less good approximation over the tidal flats where water depths are small and the deposition rates potentially high. The demanding long computational times, for the simulation of the wave conditions, prohibited a full time-step-by-time-step coupling between the hydrodynamics, sediment transport and wave modules.

Table 4 Relative occurrence of the nine combinations of classes of events over a period of 33 years

	High run-off			Medium run-off			Low run-off		
	No. of years/ 33 years	Occurrence	No. of years in 10 years	No. of years/ 33 years	Occurrence	No. of years in 10 years	No. of years/ 33 years	Occurrence	No. of years in 10 years
High waves	4/33	0.12	1	5/33	0.15	2	1/33	0.03	0
Medium waves	5/33	0.15	2	5/33	0.15	2	4/33	0.12	1
Low waves	–	–		2/33	0.06	0	7/33	0.2	2

The occurrence in the number of years for combinations of high, medium and low waves and run-off over 33 years is presented. The relative occurrence is given as well the expected number of occurrences for a period of 10 years

Table 5 Scaling factors for daily and hourly run-off calculated for all discharges above a minimum of 200 m³/s and the calibrated values applied in the morphodynamic simulations

1April/31March	Scaling daily values	Scaling hourly values	Calibrated values
1998–1999	1.18	–	0.6
1999–2000	0.8	–	0.4
2000–2001	2.93	–	1.4
2001–2002	0.95	–	0.5
2002–2003	1.3	–	0.7
2003–2004	0.9	1.02	0.45
2004–2005	0.1	0.18	0.1
2005–2006	0.5	0.6	0.25
2006–2007	1.4	1.5	0.7
2007–2008 (reference)	1	1	1
2008–2009	1.05	–	–

The scaling factors for the dam run-off are given in Table 5 (fourth column). The scaling factors are given for a year with a low, medium and high forcing. For the waves and the wind, the scaling factors are 0.7/0.8/1.0 and 0.8/0.9/1.0, respectively. The years 1998 and 2000 are characterised by a high run-off; 1999, 2001, 2002, 2003 and 2004 by a medium run-off and 2005 by a very low run-off. The waves are about high to average, except in the years 2004 and 2005, which represent years with small waves, see also Table 3. Unfortunately, no information was available for the waves and winds for the year 2002, which adds an element of uncertainty to the results.

The differential maps for 1998–2001, 2001–2003 and 2003–2005 are available for comparison with the simulations. The observations and results of the simulations are shown in Fig. 12.

For the period 1998–2001, the observations show a strong erosion not only in the internal estuary (>1 m in certain points) but also in the intermediate part (25–50 cm)

Fig. 11 Morphological update procedure from year *n* to year *n*+1

and over the Strado tidal flat to the north at the mouth of the estuary. Deposition is found north and south in the intermediate part and towards the external estuary. The strong curvature of the channel in the internal estuary indicates that the observed deposition and erosion are influenced by lateral movements due to helical flow. The simulations reproduce these erosion and deposition tendencies very nicely; however, the thickness of the deposition remains below 30 cm. A comparison in absolute values with the measured differential maps must be made with caution. These are associated with uncertainty in the order of ±25 cm and up to ±1 m near the channel where the bottom gradients are steep (Goubert, personal communication).

From June 2001 to September 2003, the system changes and the differential map shows a strong sedimentation in the intermediate and internal estuary. In the eastern part of the external estuary, sedimentation of up to 25 cm is observed. Waves and run-off are characterised as average for this period. Areas with erosion are found in the external estuary and south of the channel mouth in the intermediate part.

The simulations reproduce the tendency for accretion in the internal estuary and the eastern part of the open bay, but on the contrary in the intermediate part, the deposition occurs on the southern mudflat. The action of the waves seems to be overestimated for this period. This is believed to be due to the uncertainties related to the wave forcing for this period. As mentioned, it was difficult to define the scaling for 2002 due to the lack of both wave and wind measurements for the year. A normal year was assumed for the waves with a direction from SSE to reduce the erosion on the northern mudflat. Under all circumstances, the observed deposition on the northern mudflat is difficult to explain but could be linked with lateral movements of the channel (meandering) or small local waves generated by easterly winds, which erode the southern tidal flat and thus facilitate a redistribution. In the internal part, the model does not reproduce the meandering, which is observed in the
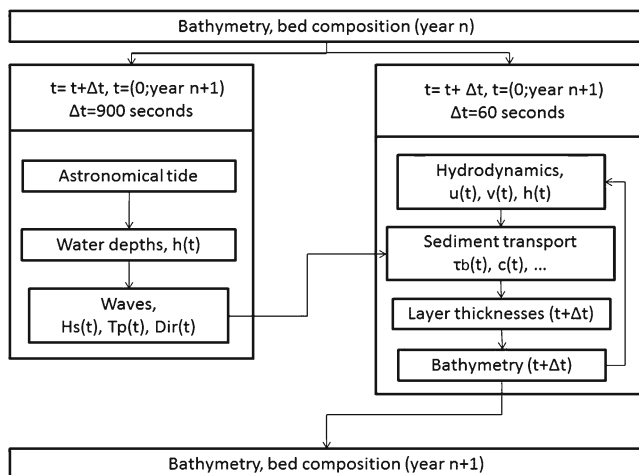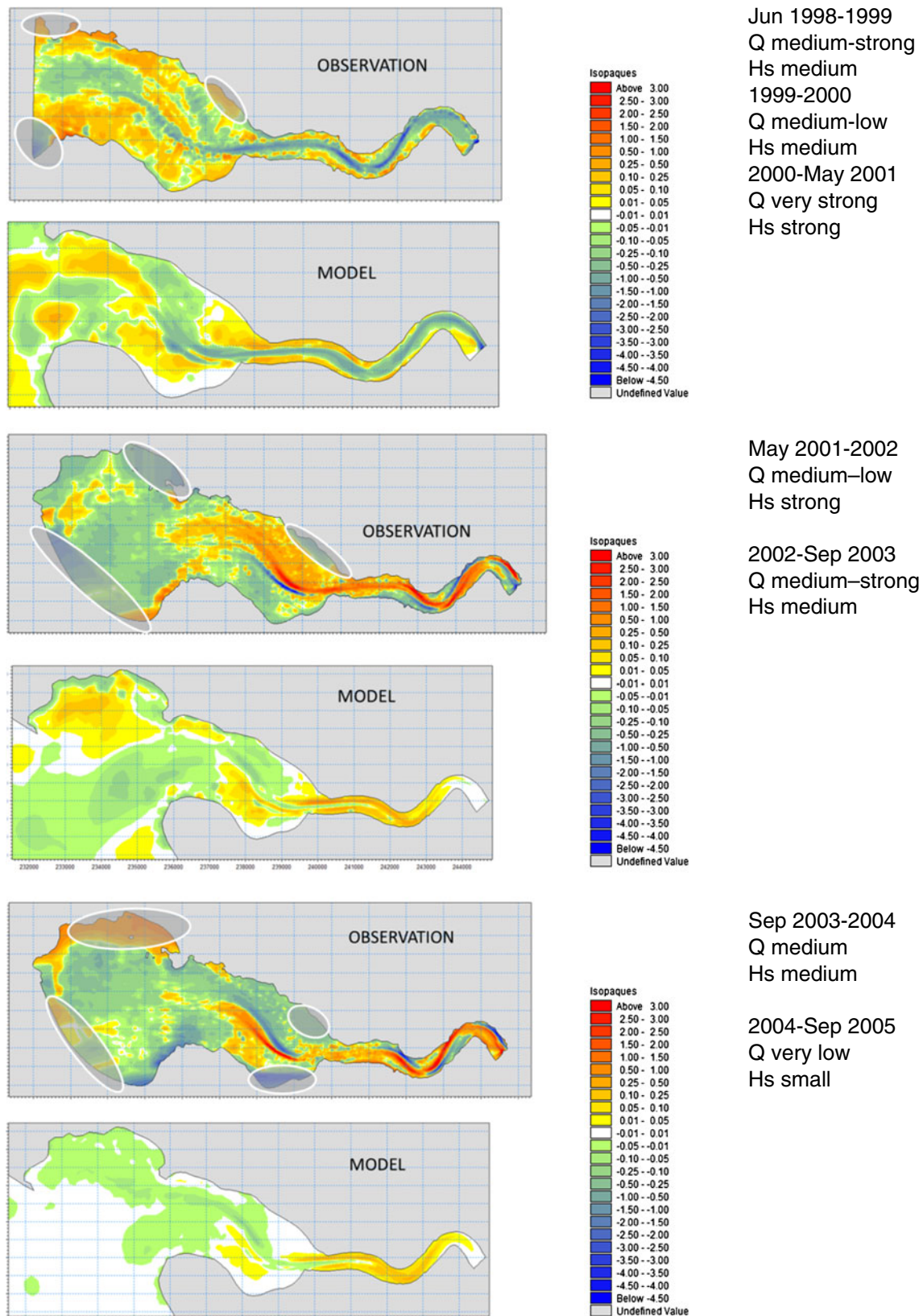
Fig. 12 Comparison of morphodynamic simulation (*lower*) and differential maps from surveys (*upper*) for the period from 1998 to 2005. Areas along coast and towards Bay of Vilaine have not been surveyed and difficulties in interpolation make the differential maps uncertain. This is indicated by hatching

Table 6 Sequence of forcing for the 10-year morphodynamic simulation with alternating high and low run-off

Year	Factor wind	Factor waves	Factor run-off
1 (reference)	1	1	1
2	1	1	0.25
3	0.9	0.8	0.7
4	0.8	0.7	0.25
5	0.9	0.8	1.1
6	0.8	0.7	0.25
7	0.9	0.8	1.1
8	1	1	0.7
9	0.9	0.8	0.7
10	1	1	0.7

The scaling factors are all relative to the reference year April 2007–April 2008

surveys, and the simulated deposition/erosion is somewhat lower.

The survey differential map from September 2003 to 2005 shows an erosion in the external estuary and deposition on the southern tidal flat. Erosion is observed on the northern mudflat in the intermediate part and deposition in the internal estuary. A displacement of the channel is observed in the internal part with locally high bathymetric changes. It is noted that the model is not designed to reproduce meandering.

The morphodynamic simulations reproduce the overall pattern, but the magnitude of deposition/erosion is lower than observed values. The absence of meandering in the model results in an underestimation of the lateral movements of the channel in the internal part. This period has relatively weak waves and average run-off, which allow for transport from the internal part to the intermediate estuary, but the run-off is not strong enough to move the sediment to the external part. The sections of the estuary that are subject to erosion are predominantly due to wave induced erosion.

The morphodynamics from 1998 to 2005 have been simulated by scaling of the reference period 2007–2008. Despite the fairly simplified scaling of the forcing, the model can reproduce the tendencies with respect to the observed spatial distributions of erosion–deposition, although with smaller amplitudes.

However, there is a disagreement in the intermediate part for 2001–2003, which may be explained by the uncertainty in the forcing for this particular period or local wave-induced erosion phenomena not resolved in the model. The formation of meandering, sometimes present in the surveys, cannot correctly be reproduced in a 2D model, as the helical flow is not included. The amplitudes in the erosion–deposition maps are thus lower compared to these occurrences. The use of a reference year scaled to reproduce hydrodynamic forcing for other years, and then applied to simulate a sequence of real historical years, means that one cannot expect to reproduce in detail the morphodynamic behaviour. However, the morphodynamic trends are reproduced confirming the applicability of the scaling.

5 Morphodynamic predictions

As illustrated, the morphodynamic model can, with a simple scaling of the reference year, reproduce realistic erosion and deposition trends over a period of 7 years. The next step is to simulate the morphodynamic behaviour of the estuary for periods of up to 10 years. The objective is to investigate the sensitivity of the behaviour with respect to initial conditions and to an extreme but historical combination of forcing event of five consecutive dry years. The underlying questions are whether there is a risk that the mouth of the estuary will silt up and whether the succession of events will maintain the equilibrium.

5.1 Scenario 1, alternating forcing

A 10-year long morphodynamic simulation has been prepared. The occurrences of high, medium and low river run-off and waves listed in Table 4 are used. The scenario has been defined to alternate between dry and wet years and respecting occurrences of the different joint events. The scaling factors in Table 6 are all relative to the reference year April 2007–April 2008. The applied scaling factors for run-off have been set to 1.1, 0.7 and 0.25 for high, medium and low, respectively.

Fig. 13 Simulated sediment fluxes of mud and sand for a year between the internal, intermediate and external estuary for a situation with high run-off (year 1). The colours show the accumulated deposition–erosion in meter at the end of the first year. Initial bathymetry is 2005
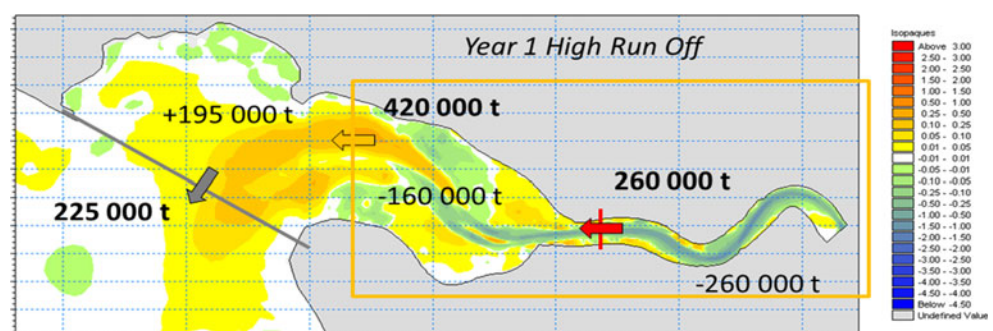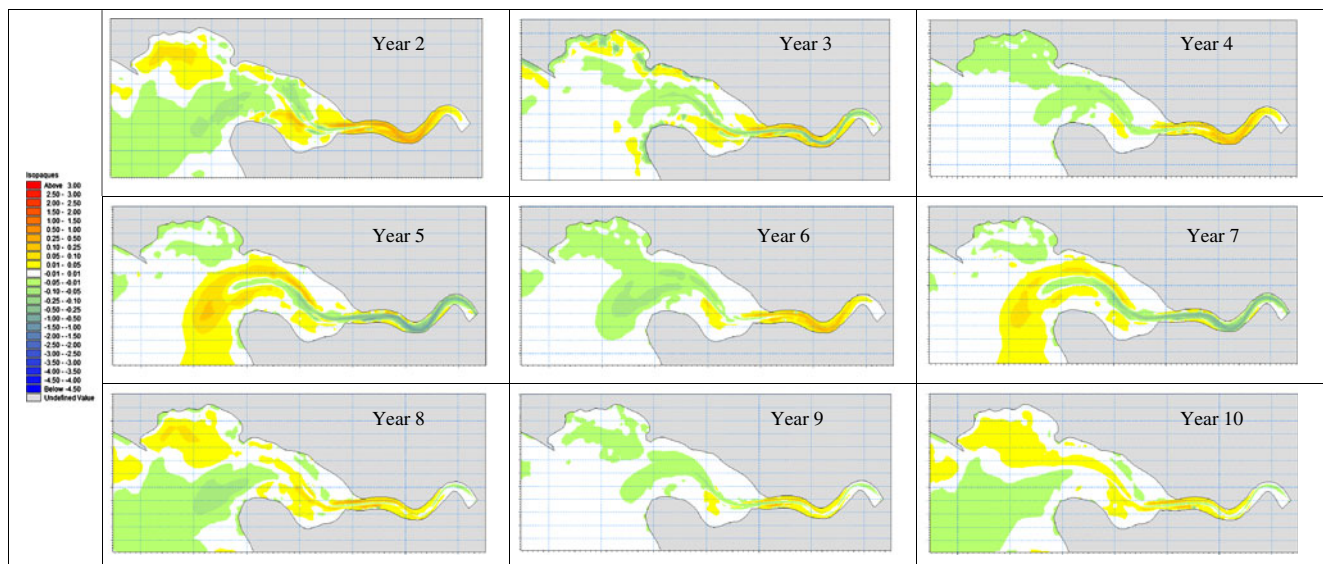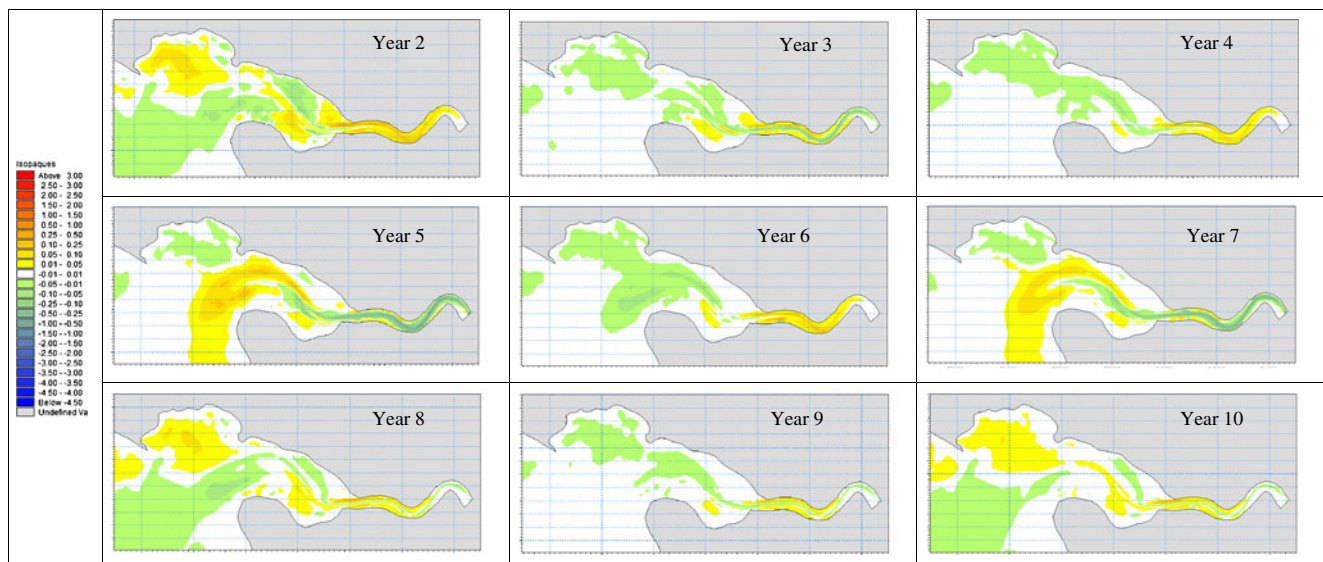
Fig. 14 Yearly deposition–erosion in metres of sediment thickness by the end of each simulation year (30 March 2008). Initial conditions year 2007

The same updating procedure is applied as for the simulations from 1998 to 2005, see also Fig. 11. The morphodynamic development may be sensitive to the initial bathymetric conditions. This was investigated by making two sets of simulation, one which starts from a shallow bathymetry (2007), and one which starts from a deeper bathymetry (2005).

The 10-year simulation starts with the reference year. Figure 13 shows the accumulated bed-thickness changes and sediment fluxes between the different compartments at the end of the first year. The high run-off during the reference year gives an export in the order of 260,000 tons from the internal part and 420,000 tons from the intermediate

part, respectively. This is well within the right order as compared with sediment fluxes of 300,000 to 500,000 tons per year calculated from bathymetric differential maps for years with a high run-off, Goubert and Menier (2005).

The yearly erosion–deposition patterns for the nine following years and starting from the bathymetry of year 2007 and 2005, respectively, are shown in Figs. 14 and 15. The years with low run-off (years 2, 4 and 6) show deposition in the internal estuary similar to the differential survey maps for 2001–2003 and 2003–2005. For the low run-off (year 2), the model predicts an import of about 120,000 tons to the internal part. This is comparable to estimates based on

Fig. 15 Yearly deposition–erosion in metres of sediment thickness by the end of each simulation year (30 March 2008). Initial conditions year 2005

observations of 100,000 to 300,000 tons, Goubert and Menier (2005).The years with high run-off (years 1, 5, and 7) erode the channel up to the mouth, which is in agreement with observations in 1994, 1995, 2001 and 2005 following a flood. The sediments are carried to the mouth and the external estuary as well as to the tidal flats in the intermediate estuary. For average run-off, the channel is erosive in the internal part, while accretion is observed on the tidal banks. The waves induce erosion in the mouth of the estuary and to the west of the Strado tidal flat, but depending on the intensity of the run-off, the erosion can be more or less compensated for by material from the internal estuary or the channel. The waves in the Bay of Vilaine generate sediment in suspension, which is advected by the tidal currents to the tidal flats, where it deposits. This is, for example, seen for year 10 with an average run-off and strong waves.

The morphodynamic fluctuations over the 10 years depend on the combination of forcing events as well as the conditions inherited from the previous year. The quantity of sediment, which is exported towards the mouth or deposits on the tidal banks, depends on the amount of sediment available in the internal estuary.

Following a dry year, the potential deposition in the external estuary is higher as a less consolidated sediment stock is available for mobilisation in the internal estuary. It is interesting to see from Figs. 14 and 15 that the influence of the initial bathymetric conditions is important in the mouth of the estuary at the beginning of the 10-year period but tends to drop off after the sixth year.

The situation after 5 years is strongly influenced by year 5, which has a high run-off. During this year, the high run-off has deepened the internal channel by 50–75 cm and generated deposits in the order of 15–20 cm at the mouth. Figure 16 shows the accumulated deposits at the end of the year 5 simulation. Relative to the initial bathymetry of 2007, erosion occurs in the internal estuary in the order of 1.5 m, and there are deposits on the banks of up to 50 cm. At the mouth and in the Bay of Kervoyal, the deposition is 15 to 20 cm. To the north of Halguen (see Fig. 1 for location), there is an erosion of 20 cm generated primarily by strong tidal currents. This is interpreted as an attempt by the tidal currents to scour a channel to return to the situation where it was deeper here, i.e. before the strong deposits, which took place in 2006–2007 and which are part of the initial conditions. If one considers the same scenario, but simulated with 2005 as the initial condition, the erosion is less pronounced, and there is a tendency for deposition here, coherent with the observations in the field.

Consolidation is simulated in its simplest form as a transition of mass from the layer above to the less erodible layers below (Teisson 1991). This transition makes the fresh deposit layer to reduce in thickness and the layer below increases in thickness. The role of consolidation is illustrated in Fig. 17, which shows the thickness of layers 2 and 3 during years 1 and 2. Two points are selected, point 1 in the mouth of the estuary and point 2 in the internal part of the estuary in the middle of the channel. The strong run-off in March of year 1 results in a large build-up of layer 2 in point 1. This coincides with an erosion of layer 3 in point 2 in the internal estuary. In the open estuary, layer 2 gradually consolidates/erodes, until it is supplied again by the winter run-offs. In the internal part, layer 2 builds up between the strong run-offs, whereupon it is eroded, as is layer 3. During year 2, layer 2 in the open estuary consolidates/erodes slowly during the year, and net changes are very small. However, in the internal part with a low run-off, there is an import by tidal flow, which results in a build-up of layer 2 with a small transition to layer 3.

Figure 17 shows that layer 2 represents the majority of the mobile sediment. Erosion of layer 3 is event driven and occurs in years with a high run-off. It acts in this respect as a source of sediment for the external estuary. With the applied values for τ_{ce} and transition rate, layer 1 is practically speaking without significance for the results.

5.2 Scenario 2, five dry years

The analysis of the historical forcing showed that it is possible to have five successive dry years. A second scenario has accordingly been constructed with a low river run-off in combination with alternating medium and weak waves, see Table 7. Dry years in combination with strong waves are very rare. Severe wave conditions are always associated with low pressure systems with storms and rains from the Atlantic.

Simulations have again been prepared for the two different initial bathymetric conditions of 2005 and 2007. After simulation of the 5 years with the 2007 bathymetry, the results show an accumulation in the internal estuary of 1.5 to 1.7 m and erosion in the estuary mouth of 10 to 20 cm, see Fig. 18. The sediment brought into suspension in the open part of the estuary deposits, apart from the internal estuary, in the Bay of Kervoyal where deposits of up to about 15 cm are found.

The simulation with the 2005 bathymetry, see Fig. 18, shows lesser erosion in the mouth of the estuary and more extended deposition. This is due to the initially deeper water here compared to the 2007 case. Consequently, less sediment is available elsewhere for deposition; this is for example visible in the internal estuary.

6 Discussion and conclusion

Given the limitations and uncertainties discussed above the morphodynamics of the Vilaine Estuary were simulated for ten successive years based on the reference year 2007–2008
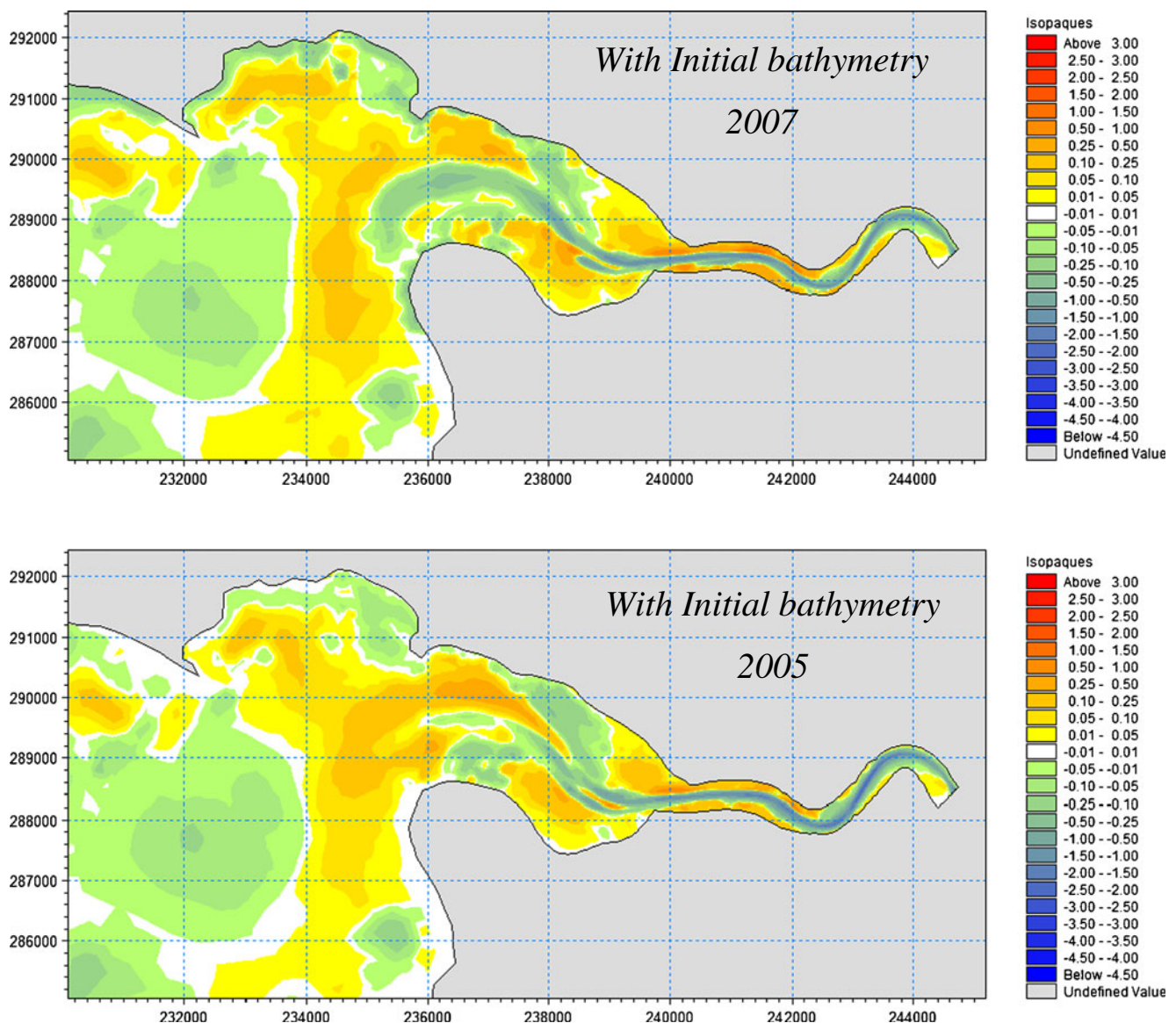
Fig. 16 Accumulated deposition and erosion after 5 years of simulation with the initial bathymetry of 2007 and 2005

with scaled forcing of wind, waves and run-off to represent low, medium and high forcing events. The application of a reference year provides a realistic high-frequency variability of the forcing and residual transport of fine particles in the estuary.

The application of a reference year to predict long-term morphology is only possible if the year has a typical combination of forcing events that can be scaled to represent the different combinations of low, high and medium forcing, i.e. is the reference year forcing scalable? The selected reference year represents a situation with strong forcing. It is shown by comparison with the differential bathymetric maps that the model can realistically reproduce both the sediment fluxes and deposition patterns. Similarly, for low river run-

off, it is shown that the reference year can be scaled to reproduce realistic sediment fluxes and deposition patterns.

The application of a scaled reference year does not take into account a variation in the sequence of events during the year from one year to another year. However, high run-off and wave conditions typically occur during the winter months. This is also the case for the selected reference year.

The relative strength of the forcing from year to year is estimated based on a measure of the annual energy. The scaling factors for run-off, however, overestimated the export of sediment from the internal to the external estuary for strong run-off and underestimated the import from the external to the internal for low run-off. It was found that in order to reproduce
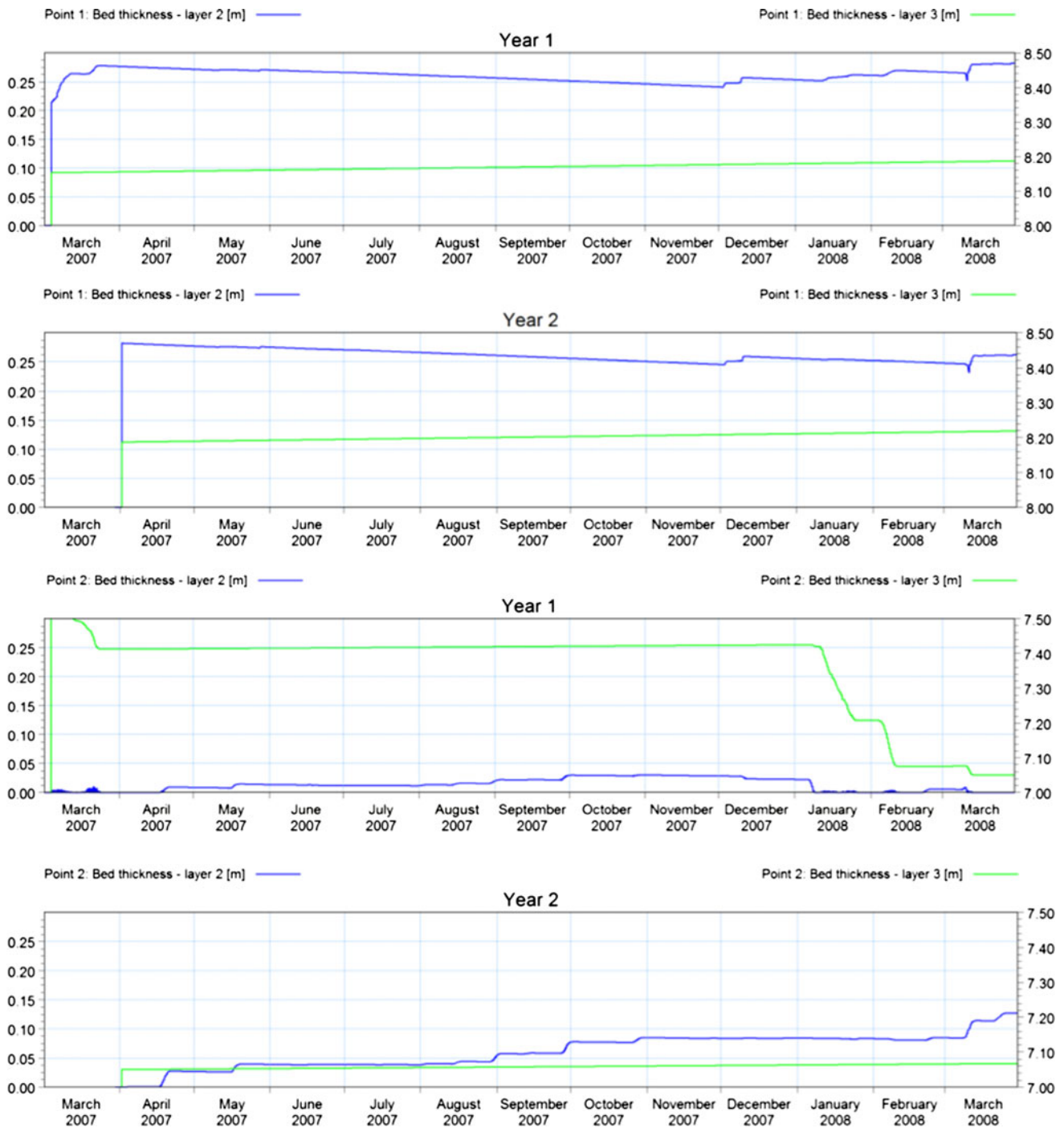
Fig. 17 Time series of the thickness of bed layers 2 and 3 during the first year and the second year. Point 1 is in the mouth of the estuary, and point 2 is in the internal part of the estuary in the middle of the channel

the morphological trends from 1998–2005, it was necessary to reduce the scaling factors, calculated from the measures of the annual energy, with respect to run-off.

The sediment eroded in the internal estuary is carried to the mouth of the estuary where it deposits. Here, it can be found several months later as seen in the observations. The mouth of the estuary is subject to strong tidal currents as well as waves

that together result in strong bed shear stresses. Despite these shear stresses, the sediment is not resuspended in nature to the extent that one would expect for freshly deposited sediment. This could be due to drag reduction not accounted for in the sediment transport model. Due to the lack of site specific near sea bed observations in the centre of Bay of Vilaine, the exact cause cannot be identified.

Table 7 Sequence of forcing for the five years morphodynamic simulation with low river run-off

Year	Factor wind	Factor waves	Factor run-off
1	1	1	0.25
2	1	1	0.25
3	0.8	0.7	0.25
4	0.9	0.8	0.25
5	0.9	0.8	0.25

It is emphasised that an accurate description of the hydrodynamics, although trivial, is crucial to be able to simulate the sediment behaviour. Cohesive sediment transport modelling of natural systems is, despite scientific progress, related with uncertainty, due to lack of understanding and correct mathematical parameterisation of the sediment processes. Model calibrations, which can reproduce short-term behaviour, are therefore not necessarily sustainable for long-term predictions. For example, bed layers may be emptied during long simulations and may starve the system for sediment, if the model is not able to build up the layers again during other forcing situations. In combination with inaccurate forcing, the model may due to non-linearity easily drift away from the expected band of results.

As the objective was to estimate the long-term morphodynamics, a relatively simple model has been developed. This is in accordance with the philosophy of Roelvink and Reniers ([2012](#)), who argue (albeit for non-cohesive coastal morphology) that adding more physics will improve
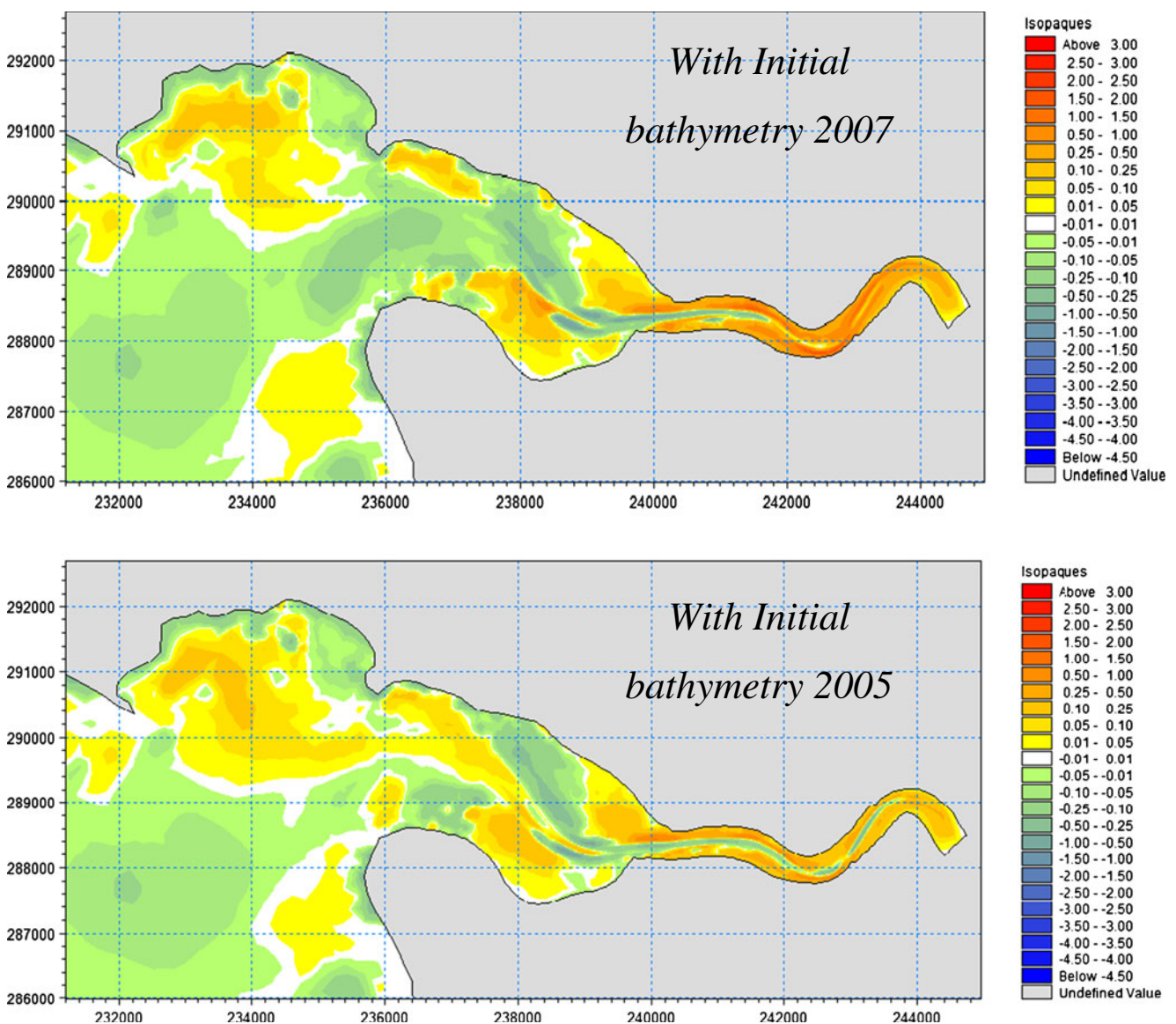
Fig. 18 Scenario 2. Accumulated deposition and erosion by the end of five dry years of simulation with the initial bathymetry of 2007 and 2005

the ability of the model to represent certain processes, but the overall model is not necessarily improved by the inclusion of physical processes, which depend on uncertain coefficients. These arguments are also valid for the simulation of the morphology of cohesive sediment environments considering the dependence on empirical data. The simplicity of the model must in any case be defined based on an analysis of the morphodynamic key processes.

With respect to the hydrodynamics, 3D effects observed during strong freshwater run-off may be required to simulate in order to reproduce the sediment movements at certain situations and locations in the main channel. On the other hand, the 2D description allowed for a high horizontal resolution, which captures the major water movements due to tidal flow, river run-off and waves. For example, it was necessary to take into account the tidal variation in order to correctly simulate the wind induced surface waves over the tidal flats and thereby the combined wave and current shear stresses.

Central in the model is the use of the Ariathurai–Partheniades equation. It scales with the square of the friction velocity and can describe both erosion from a hard seabed as well as resuspension from a soft bed (Petersen and Vested 2002), thus limiting the complexity of the model.

The key process of erosion of the deeper more resistant sea bed during extreme river run-off and deposition of this material in the external estuary, where it slowly consolidates before being resuspended by strong storm waves, could not be simulated without a layered bed description. From a long-term modelling point of view, the simulations showed that it is possible to describe the seabed processes by a three-layer description with a simple consolidation parameterisation.

The flocculation description, which scales with sediment concentrations, was necessary to reproduce the measured sediment suspensions. A constant settling velocity for the cohesive sediment was also tested, but the results were not satisfactorily.

In order to calibrate the model, horizontal maps for the critical shear stresses for deposition and erosion were applied. These maps reflect the horizontal heterogeneity of the seabed due to physical and biological conditions from the deeper parts of the estuary to the tidal flats. The use of such static parameter maps can impact the morphodynamic response of the system and can only be applied if the morphodynamic changes are small. Ideally, the parameter maps should be dynamic. For example, as a function of the water, depth and the maps should change with the morphological development. However, such a feedback into the parameter maps would complicate the model significantly. In the case of Vilaine, the morphodynamic response from year to year is relatively small.

The Vilaine Estuary is from a sediment transport modelling and open boundary condition points of view ideal as the morphology is governed by internal sediment redistribution.

It is well documented that there is no sediment input from upstream the dam. The sediment influx across the open boundary condition in the Bay of Vilaine was set to zero. Sensitivity tests showed no impact on the results within the time span of years. Off course, if the model was run for even longer time spans than 10 years, one must expect an impact on the sediment budget of this. The import of sediment to the Bay of Vilaine depends on the 3D flow, and the storm conditions and wind directions, over a larger sea area Tessier et al. (2008).

The simulations of the morphological development show a strong dependency of the initial bathymetry. In hindsight, this is not surprising. A deeper estuary is more susceptible to siltation compared to a shallower one. The response time of the system to strong hydrodynamic forcing is rather short. The simulations show that major morphodynamic changes can occur within a series of strong winter storms with high run-offs. The importance of the initial bathymetry seems to disappear after a period of about 5 years with typical alternating forcing.

To address the uncertainty in forcing due to variations in climatic conditions and weather events, one should ideally run the model for other realistic combinations of forcing as well as for different initial bathymetric conditions to provide an ensemble of possible results. These results can then be analysed statistically and the most likely morphological trends determined. Practical constraints in computational speed, however, reduce the number of simulations and do not allow such an approach.

The river run-off data were available from 1970–2009 and the offshore wave data from 1979–2002 only. The analysis of the forcing data was difficult due to lack of a longer offshore wave data record. If, at the same time, series of several years of river run-off and offshore wave height data with a time resolution of hours are available, the joint probability of river run-off and waves could be made on an event basis and not as yearly averaged. This would also allow taking into consideration the duration of events and at what time of the year they occur. As a result, one would have scaling factors that worked on events. In this way, one could have one set of scaling factors for high river run-off and strong waves, and another set for small river run-off and strong waves.

The methodology represents an alternative to a simulation procedure based on the selection of representative forcing or processes and morphological speed up factors. This is relevant in environments where, in addition to the constant tidal flow, waves and run-off conditions change from year to year, making a selection and sequence of events nontrivial.

High-resolution meteorological and hydrological hind cast data bases are constructed as part of climate research. Access to these will make it possible to define hydrodynamic forcing with consistent data for many more than the present

10 years. However, for fine sediment transport modelling, there will always be a demand for local data for both calibration and validation. Thus, a method to extend a data-rich short-term period, with all input data for initial and open boundary conditions available for the model, to longer periods is required. The application of a reference year, with scaling factors for the open boundary conditions to represent other years, is an example of this.

References

DHI (2009a) MIKE 21 & MIKE 3. Flow model FM hydrodynamic and transport module scientific documentation. DHI, Hørsholm, 50 p. Accessed March 2009

DHI (2009b). Modélisation numérique hydrosédimentaire de l'estuaire de la Vilaine. Phase 4 : Modélisation hydrodynamique. Report prepared for IAV. http://www.eptb-vilaine.fr/site/index.php/lestuaire/etudes-et-rapports/etudes. Accessed March 2009

Fredsoe J (1984) Turbulent boundary layer in a wave–current motion. J Hydraulic Engng 110:1103–1120, ASCE

Goubert E, Menier D (2005) Evolution morphosédimentologique de l'estuaire de la Vilaine de 1960 à 2003: valorisation des campagnes bathymétriques. Report prepared by UBS for IAV, 104 pp. http://www.eptb-vilaine.fr/site/index.php/lestuaire/etudes-et-rapports/etudes. Accessed November 2005

Goubert E, Frenod E, Peeters P, Thuillier P, Vested HJ, Bernard N (2010) The use of altimetric data (Altus) in the characterization of hydrodynamic climates controlling hydrosedimentary processes of intertidal mudflat: the Vilaine estuary case (Brittany, France). Revue Paralia 3:6.17–6.32

Hibma A (2004) Morphodynamic modelling of estuarine channel–shoal systems. PhD thesis, Delft University of Technology, pp 143

Jestin H, Bassoullet P, Le Hir P, L'Yavanc J, Degres Y (1998) Development of ALTUS, a high frequency acoustic submersible recording altimeter to accurately monitor bed elevation and quantify deposition or erosion of sediments, vol. 1. OCEANS '98 Conference Proceedings. pp 189–194

Latteux B (1995) Techniques for long-term morphological simulations under tidal action. Mar Geol 126:129–141

Le Hir P, Cayocca F, Waeles B (2011) Dynamics of sand and mud mixtures: a multiprocess-based modelling strategy. Cont Shelf Res 31:135–149

Lumborg U, Pejrup M (2005) Modelling of cohesive sediment transport in a tidal lagoon—an annual budget. Mar Geol 218:1–16

Mitchener HJ, Torfs H, Whitehouse RJS (1996) Erosion of mud/sand mixtures. Coast Eng 29:1–25, Errata 1997, 30, 319

Petersen O. and Vested HJ (2002) Description of vertical exchange processes in numerical mud transport modelling. In: Winterwerp C and Kranenburg C (eds) Fine sediment dynamics in the marine environment. Elsevier, Amsterdam, pp 375–393

Roelvink D, Reniers A (2012) A guide to modelling coastal morphology. Advances in coastal and ocean engineering, vol. 12. World Scientific Publishing Co. Singapore, pp 292

Sørensen OR, Kofoed-Hansen H, Rugbjerg M and Sørensen LS. (2004) A third-generation spectral wave model using unstructured finite volume technique. Proceedings of the 29th International Conference on Coastal Engineering. World Scientific, 894–906

Soulsby RL, Hamm L, Klopman G, Myrhaug D, Simons RR, Thomas GP (1993) Wave–current interaction within and outside the bottom boundary layer. Coastal Enggr 21:41–69

Teeter AM (1986) Vertical transport in fine-grained suspension and nearly deposited sediment. Estuarine cohesive sediment dynamics, lecture notes on coastal and estuarine studies, 14, Springer, Berlin, pp 126–149

Teisson C (1991) Cohesive suspended sediment transport: feasibility and limitations of numerical modelling. J Hydraul Res 29(6):755–769

Tessier C, Le Hir P, Dumas F, Jourdin F (2008) Modélisation des turbidités en Bretagne Sud et validation par des mesures in-situ. European Journal of Environmental and Civil Engineering 12(1–2):179–190

Tessier C, Vested HJ, Christensen BB, Goubert E and Salaün F (2012) Modélisation numérique de la dynamique sédimentaire de l'estuaire de la Vilaine. XIIièmes Journées Nationales Génie Côtier -Génie Civil, Cherbourg, 12–14 juin, Actes de colloques, Editions Paralia CFL, pp.471-480, doi:10.5150/jngcgc.2012.051-T

Toorman EA, Bruens AW, Kranenburg C and Winterwerp JC (2002) Interaction of suspended cohesive sediment and turbulence. In: Winterwerp JC and Kranenburg C (eds) Fine sediment dynamics in the marine environment. Elsevier, Amsterdam, pp 7–23

van Ledden M, Wang ZB, Winterwerp H, de Vriend H (2006) Modelling sand–mud morphodynamics in the Friesche Zeegat. Ocean Dyn 56:248–265

Waeles B (2005) Modelisation morphodynamique de l'embouchure de la Seine. PhD Thesis, IFREMER/Université de Caen, France, pp 230

Whitehouse R, Soulsby R, Roberts W and Mitchener H (2000) Dynamics of estuarine muds HR Wallingford & Thomas Telford, London

Winterwerp JC and Kesteren WMG (2004) Introduction to the physiscs of cohesive sediment in the marine environment. Elsevier, Amsterdam